DETERMINING LEEB HARDNESS AND ITS CONTROLLING FACTORS TO ASSESS THE STRENGTH OF SEDIMENTARY ROCKS

by

CLAYTON REINHARD FREIMUTH

Bachelor of Science, 2015
Frostburg State University
Frostburg, Maryland

Submitted to the Graduate Faculty of the
College of Science and Engineering
Texas Christian University
In partial fulfillment of the requirements
For the degree of

Master's of Science
August 2021

Acknowledgements

First, I would like to thank my advisor, Dr. Helge Alsleben, for his assistance and guidance throughout the whole process of developing this thesis. Also, I want to thank Dr. Arthur Busbey and Dr. Omar Harvey for their assistance in the statistical and mineralogical analyses, respectively. I would like to thank Dr. Richard Hanson for his assistance with the equipment in the rock prep room. Finally, I want to thank the members of the machine shop on campus for their patience and assistance in running the machines within the rock prep room.

Second, I would like to thank my friends and family for providing moral support during the thesis process. Not only was I able to collect a large portion of my samples during Anthony Skaleski's research trips to New Mexico, but he and several others (Blake Bezucha, Josh Davidson, and Shaun Prines) also provided guidance and moral support during the research process. I also want to thank my family for the support they provided me throughout this process. Despite them not having a background in geology, they were faithful listeners and provided advice where they could.

Finally, I would like to thank those whom I didn't mention specifically here. To anyone who helped me through this process thanks.

This thesis is dedicated to all of you.

Table of Contents

List of Figures

List of Tables

Chapter 1: Introduction

Purpose and Objectives

The purpose of this study was to examine the hardness of various sedimentary rocks and its relationship to selected intrinsic properties, specifically bulk mineralogy, porosity, sample volume, and density. Previous studies considered these factors individually and their univariate effects on hardness. However, to my knowledge, none has considered their collective/multivariate influence on hardness. This latter, more comprehensive approach and elucidation of multivariate constraints on the intrinsic properties controlling rock hardness is the primary focus of this study.

The study also seeks to extend current understanding of the relationship between a sample's hardness and its unconfined compressive strength (UCS). Previous studies indicate that hardness and UCS are related, but the factors governing this relationship are not well understood. It is anticipated that through this study's efforts to better constrain the intrinsic properties controlling hardness, the relationship between hardness and UCS could be better constrained. Specific objectives of the study were to: 1) determine which variables most control hardness, 2) predict UCS from hardness values, and finally 3) determine how well hardness correlates to UCS.

Background Information

Hardness, Strength, their measurement and relationship

All materials, including rocks, respond in both elastic and inelastic manner during loading. Elastic deformation occurs when a material returns to its original state after loading. However, inelastic deformation, sometimes known as plastic deformation, is

permanent and the material will not return to its original state after loading. Hardness refers to a material's resistance to surface deformation (Broitman, 2017) and is controlled by surface elasticity and energy loss due to plastic deformation properties related to a material's mechanical strength (Verwaal and Mulder, 1993; Yasar and Erdogan, 2004; Aoki and Matsukura, 2008; Asiri, 2017). In geology, material strength is typically defined as the unconfined compressive strength (UCS). UCS is the maximum stress the material can withstand before brittle failure in response to axial loading (Hudson and Harrison, 2000). Specifically, UCS is the peak stress during a load test before the material fails (Hudson and Harrison, 1997).

One instrument used to measure the hardness of a material is the Proceq Equotip Bambino (hereafter referred to as Bambino) micro-rebound hammer. Dietmar Leeb invented the Bambino in 1977 as a method for testing metal hardness. The Bambino uses a spring-loaded tungsten carbide impact body to measure the initial and rebound velocity (Figure 1; Leeb, 1979). The ratio of the initial and rebound velocity is multiplied by 1000 to obtain the Leeb hardness (Leeb, 1979). Since the Bambino's initial development, its use has spread from materials engineering to other industries such as the petroleum (Lee et al., 2014; Brooks et al., 2016; Dong et al., 2017; Colwell, 2018), mining (Okan and Momayez, 2017), and construction industries (Hack et al., 1993; Coombes et al., 2013; Szilagyi et al., 2015; Yilmaz and Goktan, 2018a; Yüksek, 2019).

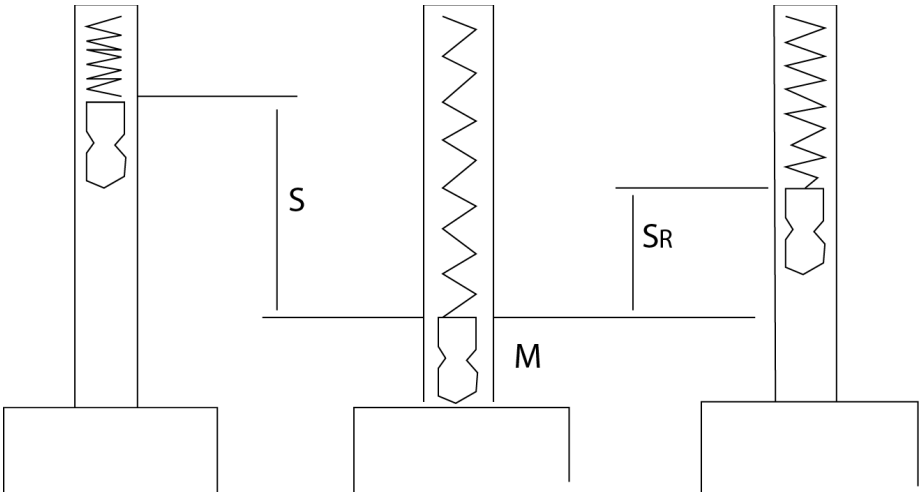

Figure 1: Mode of Bambino operation. "S" is the striking phase, "M" is the measurement phase, and "SR" is the rebound phase of operation (after Leeb, 1979).

Impact hardness and axial load testing, both apply a load to the material being tested. However, in hardness measurements the application of this load is smaller in magnitude and almost instantaneous in duration. The similarity between hardness and UCS determinations allows correlation between Leeb hardness and measured UCS values (Verwaal and Mulder, 1993; Aoki and Matsukura, 2008; Lee et al., 2014). Consequently, numerous empirical equations have been developed for predicting UCS from Leeb hardness (e.g., Verwaal and Mulder, 1993; Hack and Huisman, 2002; Shalabi et al., 2007; Aoki and Matsukura, 2008; Asiri, 2017). Reported correlations between rock hardness and its UCS are always positive (Verwaal and Mulder, 1993; Hack and Huisman, 2002; Kawasaki et al., 2002; Yasar and Erdogan, 2004; Aoki and Matsukura, 2008; Lee et al., 2014; Brooks et al., 2016; Celik and Cobanoglu, 2019), indicating that stronger samples also have higher Leeb hardness values.

Despite the positive correlation between Leeb hardness and UCS, the independent variables that control rock hardness, and ultimately rock strength, are not well understood. Golodkovskaia et al. (1975) suggest that rock strength is related to several

factors (e.g., mineral composition and texture), but they do not link these factors to hardness. Other methods either measure UCS, or predict it from hardness by focusing on the correlation between the two, without considering all potential controlling properties (Verwaal and Mulder, 1993; Kawasaki et al., 2002; Aoki and Matsukura, 2008; Yilmaz and Goktan, 2018a; Celik and Cobanoglu, 2019). The limitation of this approach lies in the fact that rocks are heterogeneous and inherent variation (e.g., bulk mineralogy, porosity, sedimentary structures, and grain size) dictates the correlation between hardness and UCS, which will inevitably vary in a sample set.

Controls on Rock Hardness

Rock hardness has been related to a number of intrinsic properties including sample volume (Viles et al., 2011; Brooks et al., 2016; Desarnaud et al., 2019), grain size (Daniels et al., 2012; Brooks et al., 2016), bulk mineralogy (Verwaal and Mulder, 1993; Kawasaki et al., 2002), porosity (Aoki and Matsukura, 2008; Brooks et al., 2016), cementation (Daniels et al., 2012; Coombes et al., 2013), the degree of weathering (Hack et al., 1993; Verwaal and Mulder, 1993; Coombes et al., 2013; Hansen et al., 2013), moisture content (Viles et al., 2011; Desarnaud et al., 2019) and sedimentary structures (Daniels et al., 2012; Brooks et al., 2016). The degree to which each independent variable control hardness is not well understood, but has been examined in various studies (e.g., Celik and Cabonoglu, 2019).

I. ***Sample Volume & Minimum Sample Thickness:***

A sample's thickness and volume can affect Leeb hardness values because of how the Bambino operates (Viles et al., 2011; Lee et al., 2014; Brooks et al., 2016; Desarnaud et al., 2019). The Bambino's depth of investigation is approximately 5 mm, due to the

tool's 11 N mm energy (Hack et al., 1993). Thus, samples require a minimum thickness of 5 mm to avoid energy dissipation at the sample-surface interface (Hack et al., 1993, Brooks et al., 2016). Other researchers suggest that a minimum thickness of 50 mm is needed to produce accurate Leeb hardness readings (Verwaal and Mulder, 1993; Kawasaki et al., 2001).

Previous researchers note that hardness also varies with volume (Demirdag et al., 2009; Lee et al., 2014; Brooks et al., 2016). Brooks et al. (2016) found that hardness values can fluctuate below 197 cm^3, due to the proximity of free surfaces, which may dissipate impact energy. To reduce erroneous measurements, Brooks et al. (2016) suggest analyzing samples of at least 197 cm^3, although others determined smaller minimum volumes (Taylor, 2017; Colwell, 2018). Based on these studies, there are some basic constraints on sample volume and thickness, but rather large uncertainties remain whether these values are universally applicable.

II. ***Grain Size:***

The impact body of the Bambino has a surface area of 7.07 mm^2 and tests a fairly small volume of rock (Hack et al., 1993; Daniels et al., 2012; Desarnaud et al., 2019). Thus, researchers hypothesize that the Bambino is sensitive to grains with surface areas larger than 7.07 mm^2 and a thickness greater than 5 mm (Hack et al., 1993, Daniels et al., 2012). In those cases, Leeb hardness values would reflect the internal hardness of these grains rather than the hardness of the rock as a whole (Hack et al., 1993, Daniels et al., 2012). Daniels et al. (2012) noted this when poorly cemented sandstone yielded high Leeb hardness due to its large quartz grains. Further research is necessary to examine the

role grain size plays in Leeb hardness, but overall care must be taken in the sampling procedure to fully characterize the true hardness of the rock sample.

III. ***Bulk Mineralogy***

Bulk mineralogy affects hardness because different minerals resist surface deformation differently (Verwaal and Mulder, 1993; Daniels et al., 2012; Ritz et al., 2014; Dong et al., 2017, Celik and Cobanoglu, 2019). Verwaal and Mulder (1993) note that bulk mineralogy controls sample hardness; rocks with higher quartz or calcareous content have higher Leeb hardness than those with higher clay content. Celik and Cobanoglu (2019) also reported different hardness across mineral type, indicative of different inherent hardness. Daniels et al. (2012) measured abnormally high hardness values in coarse-grained, poorly cemented sandstones. These high Leeb values led Daniels et al. (2012) to predict high UCS values, but further UCS testing returned low values, which was attributed to poor cementation. Daniels et al. (2012) hypothesized that the higher Leeb hardness reflects the hardness of quartz grains, which only partially controls the strength of the whole rock sample.

IV. ***Porosity***

Porosity can affect rock hardness because pores dissipate impact energy similar to the sample-surface interface (Aoki and Matsukura, 2008; Brooks et al., 2016). Aoki and Matsukura (2008) were the first to examine total porosity and its effect on rock hardness. Brooks et al. (2016) did the same in their later study. Based on these studies, samples with higher porosity dissipate more of the impact energy, whereas low porosity materials do the opposite. However, the exact magnitude of this effect is not known and additional

work is needed to quantify the effects of porosity. Specifically, more work is needed to determine whether total porosity or pore size distribution controls hardness.

V. ***Sedimentary Structures***

Sedimentary structures can influence Leeb hardness (Brooks et al., 2016). In their study, Brooks et al. (2016) focused primarily on laminations and bioturbation. Bioturbation in samples can cause large scattering in Leeb hardness (Brooks et al., 2016). Daniels et al. (2012) report that individual laminations in a core can have highly variable Leeb hardness values as well. Sedimentary structure geometries could influence how the impact energy travels through a sample. Brooks et al. (2016) provide an example with their work comparing bioturbated carbonate rocks to non-bioturbated rocks. Comparing the hardness of rocks with similar lithologies, but different sedimentary structures, is one potential method to address this question.

VI. ***Cementation***

Cementation affects rock hardness in two ways: the amount of cement present, and the mineralogy of the cement. Coombes et al. (2013) examined how weathering of limestones and concrete samples affects resulting hardness. The researchers found limestone hardness decreased, corresponding to dissolution of cement during weathering (Coombes et al., 2013). However, concrete samples from the same experiment were further cemented by mineral precipitation from seawater (Coombes et al., 2013). As a result, the hardness of the concrete increased (Coombes et al., 2013). Daniels et al. (2012) also discuss the possibility of abnormal hardness values due to resin cements in laboratory samples. Based on these studies, cementation type and amount must be considered during hardness testing.

VII. ***Degree of Weathering***

The degree of weathering controls sample hardness because weathering can alter the grains and cementation of a rock (Viles et al., 2011; Coombes et al., 2013; Hansen et al., 2013; Wilhelm et al., 2016). Verwaal and Mulder (1993) noticed differences in hardness between weathered dolomite and fresh dolomite; weathered dolomites returned lower hardness than fresh samples. Similarly, Hack et al. (1993) observed lower hardness values in weathering rinds and that cutting these away to unaltered faces resulted in higher hardness values. Although weathering can reduce the absolute hardness values, the degree of weathering and related hardness values can be useful. Alberti et al. (2013) utilized the hardness of weathered rocks to correlate river terrace deposits in Spain. However, the purpose of this study is to measure the true hardness of a sample. Therefore, any weathering rinds were removed prior to hardness testing.

VIII. ***Moisture Content***

Like weathering and porosity, moisture content can negatively affect hardness values (e.g., Desarnaud et al., 2019). Desarnaud et al. (2019) measured a drop in hardness between 13% and 17% as corresponding moisture content increased between 5% to 12% (Desarnaud et al., 2019). This could potentially lead to erroneous measurements of Leeb hardness, as well as poor UCS predictions. Desarnaud et al. (2019) used ovens to dry their samples over a period of 24 hours, thus decreasing moisture content. Aoki and Matsukura (2008) allowed their samples to air dry before testing. Both methods appear equally valid for ensuring moisture content will not affect measurements, although a statistical comparison of results from these two methods has not been conducted.

Statistical Methods

Many statistical relationships between rock hardness and strength exist in the literature because there is no standardized formula relating the two. The linear correlation between hardness and strength is the most common method used to relate the two properties (Verwaal and Mulder, 1993; Kawasaki et al., 2002; Aoki and Matsukura, 2008; Yilmaz and Goktan, 2018a; Celik and Cobanoglu, 2019). These correlations seek to predict rock strength based solely on rock hardness, thus making these equations expedient (Verwaal and Mulder, 1993; Kawasaki et al., 2002; Aoki and Matsukura, 2008; Yilmaz and Goktan, 2018a; Celik and Cobanoglu, 2019). However, these correlations often eliminate outliers in the dataset to make use of parametric statistics. As Wilhelm et al. (2016) discuss, outliers are natural variations within a system and thus should not be discounted. Instead, researchers should use robust non-parametric statistics because these will not skew towards outliers (Wilhelm et al., 2016). Other approaches are exploratory and consider the role of independent variables in a sample (Grima and Babuska, 1999; Meulenkamp and Grima, 1999; Manouchehrian et al., 2012). The primary methods used in exploratory studies are: multivariate regression, artificial neural networks, and fuzzy logic (Grima and Babuska, 1999; Meulenkamp and Grima, 1999; Manouchehrian et al., 2012). Exploratory approaches accommodate natural variations in samples, but may not be suitable for rapid field estimations due to the amount of time and data needed to properly develop them (Daniels et al., 2012). Therefore, deciding which statistical technique is appropriate is another goal of this study.

I. Linear Correlation:

Linear correlation between rock hardness and rock strength is a common method in the literature because it allows researchers to predict UCS from only sample hardness, thus making it expedient (Verwaal and Mulder, 1993; Kawasaki et al., 2002; Aoki and Matsukura, 2008; Yilmaz and Goktan, 2018a; Celik and Cobanoglu, 2019). This technique compares sample hardness to the corresponding sample strength and fits a linear equation to a group of data points (Verwaal and Mulder, 1993; Kawasaki et al., 2002; Aoki and Matsukura, 2008; Yilmaz and Goktan, 2018a; Celik and Cobanoglu, 2019). However, an issue with this method is that other important independent variables controlling hardness are ignored (e.g., bulk mineralogy, porosity). Therefore, the range of predicted UCS values can be quite large (Meulenkamp and Grima, 1999; Kawasaki et al., 2002; Aoki and Matsukura, 2008; Lee et al., 2014). Additionally, outliers are often eliminated because they skew the data (Aoki and Matsukura, 2008; Alberti et al., 2013; Wilhelm et al., 2016; Colwell, 2018). This is problematic because outliers are part of the natural variation in a system and should not be ignored (Wilhelm et al., 2016).

II. Parametric vs. Non-Parametric Statistics:

Parametric statistics are used when datasets are normally distributed. Thus, these methods are sensitive to outliers in the data (Grima and Babuska, 1999. Consequently, many researchers trim the outliers in order to use parametric statistics (Aoki and Matsukura, 2008; Alberti et al., 2013; Colwell, 2018). One way to circumvent eliminating outliers is to use median values because they are not as sensitive to outliers as mean values (Yilmaz and Goktan, 2018b). Wilhelm et al. (2016) propose using non-parametric statistics because they are more robust and less influenced by outliers in the

sample data. Therefore, non-parametric statistics may better reflect a sample's composite hardness, but comparing parametric and non-parametric methods is necessary to determine which is superior.

III. Exploratory Methods:

Other statistical techniques include multivariate exploratory methods, which involve examining a dataset and the relations between variables, not necessarily testing assumptions. Multivariate exploratory methods include: multiple regression, principal components analysis, artificial neural networks, and fuzzy logic (Grima and Babuska, 1999; Meulenkamp and Grima, 1999; Tiryaki, 2008; Manouchehrian et al., 2012; Rezaei et al., 2012). All exploratory methods are similar in their aim, but differ in execution. These methods differ from standard statistics because they accommodate the natural variation in datasets. Thus, outliers and natural variations can be more easily explained via these methods.

Multiple regression analysis is a method that examines and eliminates input variables based on how much they contribute to an output. This method requires careful analysis of the significance of each independent variable against an output. Meulenkamp and Grima (1999) developed an equation using multiple regression during their study on artificial neural networks. The purpose of the equation was to check the validity of the artificial neural network (Meulenkamp and Grima, 1999). The equation relied on the following independent variables: porosity, grain size, and density, and had an R^2-value greater than 0.9, indicating a good fit between the equation and dataset (Meulenkamp and Grima, 1999).

Principal components analysis (hereafter, PCA) is similar to multivariate regression analysis but differs because it finds natural groups in datasets. These natural groupings of variables allow the development of better predictive models (Tiryaki, 2008). The result of PCA is a more homogenous data set, where certain variables driving the input-output relationship are identified and grouped (Tiryaki, 2008). Therefore, most PCA models reduce the number of controlling variables from all possible variables to a handful of dominant ones.

While multiple regression and PCA are both methods to determine the independent variables controlling rock hardness, Meulenkamp and Grima (1999) find that an artificial neural network is superior. Meulenkamp and Grima (1999) draw this conclusion because the artificial neural networks had higher R^2 values than the multiple regressions. The regression model had R^2-values of 0.957 and 0.906 for two test sets whereas the artificial neural network had R^2-values of 0.967 and 0.962 for the same sets, indicating superiority in prediction capabilities (Meulenkamp and Grima, 1999). While the neural networks were superior to multiple regression models, neither were bad because the R^2-values are greater than 0.9, indicating high correlation.

Fuzzy logic is a method of determining input-output relationships using approximations (Grima and Babuska, 1999; Rezaei et al., 2012). In a way, fuzzy logic is very similar to multiple regression analysis, but is more rigid because it is a formal model. The results are described as "good enough" solutions to a problem (Grima and Babuska, 1999; Rezaei et al., 2012). In their 1998 study, Grima and Babuska used the Takagi-Sugeno fuzzy method to predict UCS and find it superior to multivariate statistical analyses. Like artificial neural networks, fuzzy logic examines data, but differs

because it does not rely on training algorithms, which are very time consuming (Grima and Babuska, 1999). Fuzzy logic relies on user determination of input variables and development of a model that returns an output variable (Grima and Babuska, 1999). Often this requires prior knowledge of important variables in a system (Grima and Babuska, 1999).

Exploratory methods are superior predictors of UCS because they account for the natural variation in rocks, rather than predicting hardness via mean values (Grima and Babuska, 1999; Meulenkamp and Grima, 1999; Tiryaki, 2008; Manouchehrian et al., 2012). However, the major drawback to using exploratory methods is that these techniques require multiple independent variables, careful calibration, and prior knowledge of the important controls (Aoki and Matsukura, 2008). Therefore, these methods are time intensive and may not be suitable for fieldwork where quick answers are necessary. Despite these issues, exploratory methods are superior in their handling of test data and their predictive capabilities, often times having much higher R^2-values than other statistical methods.

Chapter 2: Methods

Sample Collection

This thesis is based on samples collected on seven different trips to Colorado, New Mexico, Oklahoma, and Texas between Fall 2019 and Spring 2020. Various rock samples were collected from different locales on each trip (Figure 2). Sample locations were selected prior to a given trip after consultation of various sources to assist in lithological identification and the targeting of certain outcrops to bolster my database.

For each sample, in addition to labelling, the GPS location (latitude and longitude), the relative location of the sample in an outcrop, and the lithology were recorded. Sample labelling included the state where the sample was collected, the trip name, and the order in which the sample was collected on that trip. All pertinent information was entered into a database containing: sample name, location, and lithology (Table 1). Other databases have different data depending on the analysis.

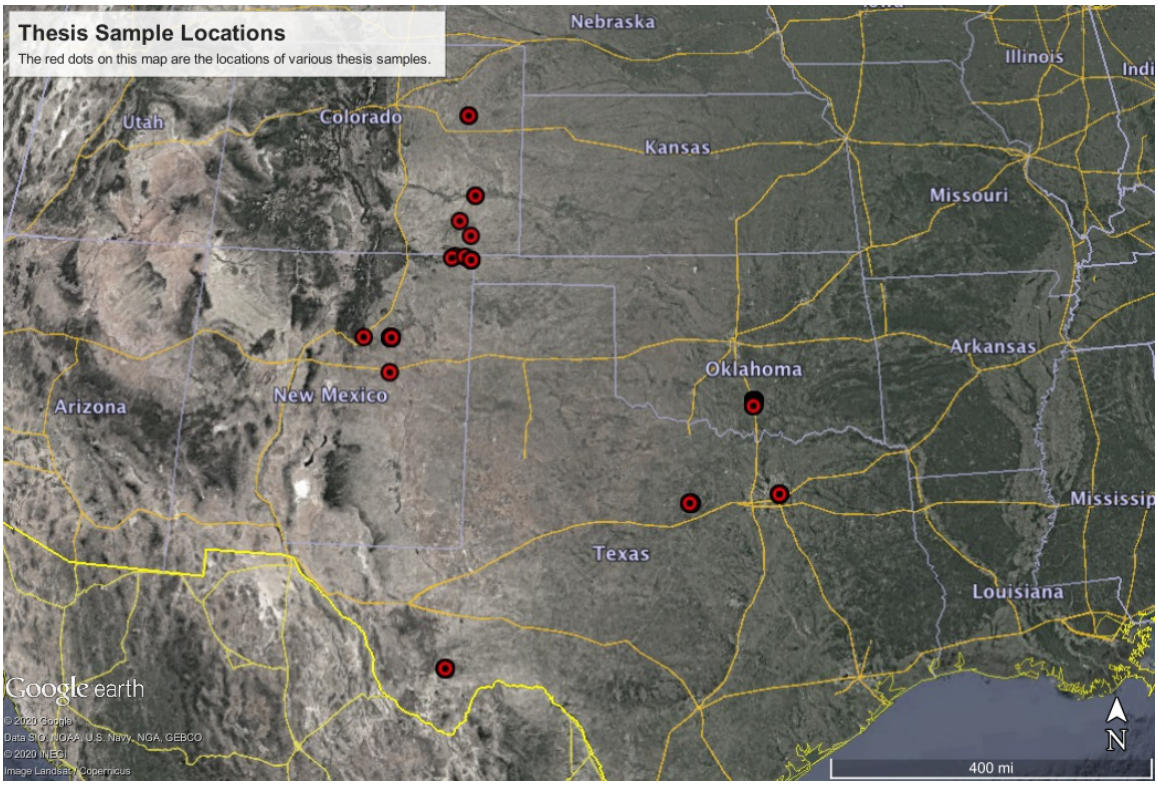

Figure 2: A map of the various sample locations used for this study.

Table 1: Summary table of each sample used in the study. The variables included here are: sample name, location, and lithology. Lithology abbreviations are: Ck=chalk, Cngl=conglomerate, LS=limestone, Mdrck=mudrock, Nvc=novaculite, Sh=shale, SS=sandstone, St=siltstone.

Sample Name	Latitude	Longitude	Lithology
COT1-1	38.0702	-103.0199	SS
COT1-2	38.0702	-103.0199	SS/Mdrck
COT1-4	39.5759	103.2674	SS
COT1-5	37.3394	-103.0822	Ck
COT1-6	39.5759	103.2674	St
NMA1-1	36.9058	-103.0508	SS
NMA1-10	35.5145	-104.6882	LS
NMA1-11	35.5151	-104.6782	SS
NMA1-12	35.5151	-104.6782	Mdrck
NMA1-14	35.5141	-104.6687	SS
NMA1-15	35.5138	-104.6668	SS
NMA1-16	35.5094	-105.2584	Cngl
NMA1-2	36.9058	-103.0508	SS/St
NMA1-3	36.9058	-103.0508	Sh
NMA1-5	36.9377	-103.4696	Cngl
NMA1-7	35.5145	-104.6882	St/Sh
NMA1-8	35.5145	-104.6882	LS
NMA1-8 Duplicate	35.5145	-104.6882	LS
NMA1-9	35.5145	-104.6882	LS
NMA1-9 Duplicate	35.5145	-104.6882	LS
NMA2-1	34.9167	-104.6552	St
OKST1-1	34.3684	-97.1388	SS/St
OKST1-10	34.4449	-97.1314	Mdrck
OKST1-11	34.4449	-97.1314	Sh
OKST1-12	34.4449	-97.1314	Sh
OKST1-13	34.4449	-97.1314	Sh
OKST1-14	34.4449	-97.1314	Sh
OKST1-15	34.4346	-97.1311	St/Sh
OKST1-15	34.4346	-97.1311	St/Sh
OKST1-17	34.4351	-97.1305	Sh
OKST1-17 (Part)	34.4351	-97.1305	Sh
OKST1-18	34.4351	-97.1305	Sh
OKST1-18	34.4351	-97.1305	Sh
OKST1-2	34.3684	-97.1388	LS

Sample Name	Latitude	Longitude	Lithology
OKST1-3	**34.3684**	**-97.1388**	LS
OKST1-4	**34.3508**	**-97.1472**	LS
OKST1-5	**34.3508**	**-97.1472**	LS
OKST1-6	**34.3786**	**-97.1428**	Ck
OKST1-7	**34.3786**	**-97.1428**	LS
OKST1-8	**34.3786**	**-97.1428**	LS
OKST1-9	**34.4269**	**-97.1329**	Cngl
TXBB1-1	**30.0399**	**-103.2806**	Nvc
TXBB1-2	**30.0399**	**-103.2806**	Nvc
TXBB1-3	**30.0399**	**-103.2806**	Nvc
TXDA1-1	**32.8544**	**-96.7174**	LS/Ck
TXDA1-2	**32.8544**	**-96.7174**	LS/Ck
TXDA1-3	**32.8544**	**-96.7174**	LS/Ck
TXPK1-1	**32.7473**	**-98.4955**	LS
TXPK1-2	**32.7496**	**-98.5284**	LS
TXPK1-3	**32.7496**	**-98.5284**	LS
TXPK1-4	**32.7470**	**-98.4967**	LS

Slabbing

After sample collection, samples were cut to volumes no less than 197 cm^3 as discussed in Brooks et al. (2016). Two faces were cut on each block: one perpendicular to bedding, and one parallel to bedding. Initial cuts were made using a 24-inch oil-lubricated rock saw (Figure 3) and trim cuts were made with a 10-inch trim saw (Figure 4). Trim cuts removed weathering rinds, created larger testing surfaces for the Bambino, and created more regular geometries. The cutting approach was found to 1) maximize the sample volume available for testing across a wide range of sample geometries and, 2) allow for assessing hardness anisotropy across two orthogonal directions.

Figure 3: Image of the large (24-inch) rock saw present in the rock prep room**.**

Figure 4: Image shows the medium (10-inch) rock saw present in the rock prep room**.**

Measurement of Mechanical Hardness

Sample holder and Bambino calibration

Prior to testing samples with the Bambino, sample holders were tested to determine which would yield the most accurate hardness values. The goals of testing various sample holders were to: minimize free surfaces, minimize the influence of other surfaces, and also return the most accurate values during hardness testing. Excess free space leads to erroneous hardness values as shown by Yilmaz and Goktan (2018b), who report that cradles with U-shapes return higher hardness values than V-shaped cradles for the same core samples.

Several mounting methods were tested including: a flat table top, a vise, a sandbox, a steel block clamped to the aforementioned table, a steel block resting on a

layer of cardboard and the table, and a steel block on top of a wood block. The tabletop method provides the easiest way to mount a sample; the sample merely rests on the tabletop. The vise has the advantage of potentially minimizing the effect of the underlying surface hardness on measurements. The sandbox was chosen to determine if a sample surrounded by other material would yield accurate values. The clamped tabletop method theoretically minimizes free surface effects between the sample and underlying surface, whereas the cardboard and woodblock methods tested whether or not a softer substrate between the sample and tabletop would yield accurate values. In testing each method, the calibration block accompanying the Bambino was secured using the respective method. The Bambino was then used to measure the hardness of Side A and B of the calibration block. A total of 20 measurements were made per method with the median hardness of each method compared to the manufacturers calibrated values of 768 and 769 HLD for Side A and B, respectively (Figure 5). Twenty measurements were selected based on previous work by Corkum et al. (2018) and Celik and Cobanoglu (2019), which showed that ≥20 impacts resulted in a margin of error that was negligible.

Based on ASTM standards (ASTM-A956-06; 2006), the Bambino is calibrated if the arithmetic mean of two tests falls within ±6 HLD of the engraved value on a calibration block. Previous research (e.g., Wilhelm et al., 2016; Yilmaz and Goktan, 2018b) found that median values should provide a more robust interpretation of the hardness data. Thus, median values were calculated and compared along with mean values to the manufacturer's provided hardness to determine the best mounting method.

Figure 5: Image shows the steel calibration block and the hardness of each face as determined by Proceq**.**

Measurement of Mechanical Hardness in rocks

Mechanical hardness in rock samples were measured using the Bambino with samples secured in a vise. Ideally, the Bambino is used on a flat, horizontal surface. To achieve this, a handheld bubble level was used to ensure that the sample was level. For irregularly shaped rocks, paper towels were used to help secure and prop up the rock when needed. After leveling a sample, the vise was hand tightened until the sample was secured such that the sample position/leveling did not change under vigorous agitation. Once sample stability and levelling were ascertained in the vise, mechanical hardness was measured across the flat surface using the single impact method (Verwaal and

Mulder, 1993; Aoki and Matsukura, 2008). Mechanical hardness measurements were made at 20 points perpendicular and 20 points parallel to bedding planes. These measurements facilitated the assessment of a hardness anisotropy index. The hardness anisotropy index is modelled after the strength anisotropy index of Soroglou and Tsiambaos (2007). Soroglou and Tsiambaos (2007) suggested that point load tests on 50 mm diameter core specimens yielded an anisotropy index value based on:

$$\mathbf{I_{(a)50}=I_{s(50)}\perp/I_{s(50)}//,}$$

where $I_{a(50)}$ is the anisotropy index for a 50 mm core specimen, $I_{s(50)}\perp$ is the point load strength of a 50 mm core specimen during axial loading, and $I_{s(50)}//$ is the point load strength of a 50 mm core specimen during diametral loading. The values for this index range from 1.0 (isotropic) to >4 (very highly anisotropic). The equation for the strength anisotropy index can be reconfigured as a hardness anisotropy index to reflect the ratio of hardness values such that:

$$\boldsymbol{I(a) = HLD(m)\perp/HLD(m)//,}$$

where $HLD_{(m)}\perp$ is the median hardness value perpendicular to bedding (pre-dry and post-dry), and $HLD_{(m)}//$ is the median hardness value parallel to bedding. A completely isotropic sample will have an anisotropy value of 1 because perpendicular and parallel hardness will be equal. If perpendicular hardness is much greater than parallel hardness, the anisotropy value is much greater than 1. Conversely, a sample with parallel hardness greater than perpendicular hardness will have a value less than 1.

Measurements were conducted on air- and oven-dried rock samples allowing for assessment of moisture content effects on hardness and anisotropy of measurements. Air-dried samples were obtained by drying field collected samples at room temperature for at

least 48 hours. Oven-dried samples were obtained by further drying air-dried samples (after measuring their hardness and mass) at 80^{o}C for 120 hours. After oven-drying, the mass of each rock and the initial air-dried mass were used to calculate the percent change in moisture content pre- versus post-oven drying.

Density, Effective Porosity and Unconfined Compressive Strength

Rock density, effective porosity and unconfined compressive strength were determined from either cylindrical core samples or rectangular plugs. Cylindrical cores were obtained using a GCTS radial arm drill press (Figure 6). Parameters for the radial drill press was set based on the hardness values from mechanical hardness testing. Generally, two samples per rock were cored unless the rock was too hard or soft, making recovery difficult. In cases where samples were too friable to core with the radial arm drill press, rectangular plugs were cut from the larger rock samples using both a 10-inch trim saw and a smaller trim saw for precision cuts.

Both the determination of density and effective porosity require mass and volume of the cylindrical cores or rectangular plugs. Mass was determined directly by weighing the samples on a digital balance. Volume of the cores and plugs were determined by adding de-ionized (hereafter DI) water to a graduated cylinder, recording the volume of DI, placing the core/plug into the graduated cylinder of DI water, and then calculating the change in volume, which is equal to the volume of the core/plug. The mass of the core/plug divided by the induced change in volume in the graduated cylinder of DI water gives the rock density. For effective porosity, the core/plug was left immersed in DI water for 120 hours (Aghamelu and Amah, 2017). After 120 hours, cores/plugs were

removed, gently dried with a paper towel, weighed and oven-dried at 80°C for 120 hours. Effective porosity of each sample was then calculated using the method described in published literature (Manger, 1963; Kawasaki, 2002; Aghamelu and Amah, 2017):

$$\boldsymbol{\Phi_{eff}=[(m_{saturated} - m_{dry})/\rho_{water}]/V_{core},}$$

where Φ_{eff} is the effective porosity, $m_{saturated}$ is the saturated mass (g) of the core in grams, m_{dry} is the dry mass (g) of the core in grams, ρ_{water} is the density of DI water (1.0 g/cm^3), and V_{core} is the volume of the core sample (cm^3).

The water immersion porosimetry technique used in this study has the advantage of being suitable to the large number of samples used as well as not requiring the specialized equipment required by alternative approaches such as gas porosimetry or mercury porosimetry.

Figure 6: The radial arm core drill used for coring samples**.**

Unconfined compressive strength measurements require samples with a 2:1 to 2.5:1 height to diameter ratio (Hoek, 1977; ASTM-D7012, 2010; Tuncay and Hasancebi, 2009; Tuncay et al., 2019). Prior to UCS measurements, cores were trimmed (using a small trim saw) to meet this criterion and to ensure that core ends were perpendicular to the core axis. Perpendicular ends would minimize errors in UCS measurements by ensuring the load cell would exert an evenly distributed load throughout the core.

A GCTS uniaxial load cell (Figure 7) equipped with a Morehouse load cell gauge was used to measure UCS for each sample. GCTS load cell operations are posted on the control panel (Figure 8). The load cell adds load to samples using an internally housed pneumatic pump, increasing the load on the plugs by 5 pounds force (lbf) per pump. Sample failure is indicated by a drop in gauge reading from peak (maximum load) value to baseline. The maximum load is recorded and used to calculate the UCS.

Figure 7: The GCTS load cell used in this study. The Morehouse force gauge is located in the upper left-hand part of the control panel.

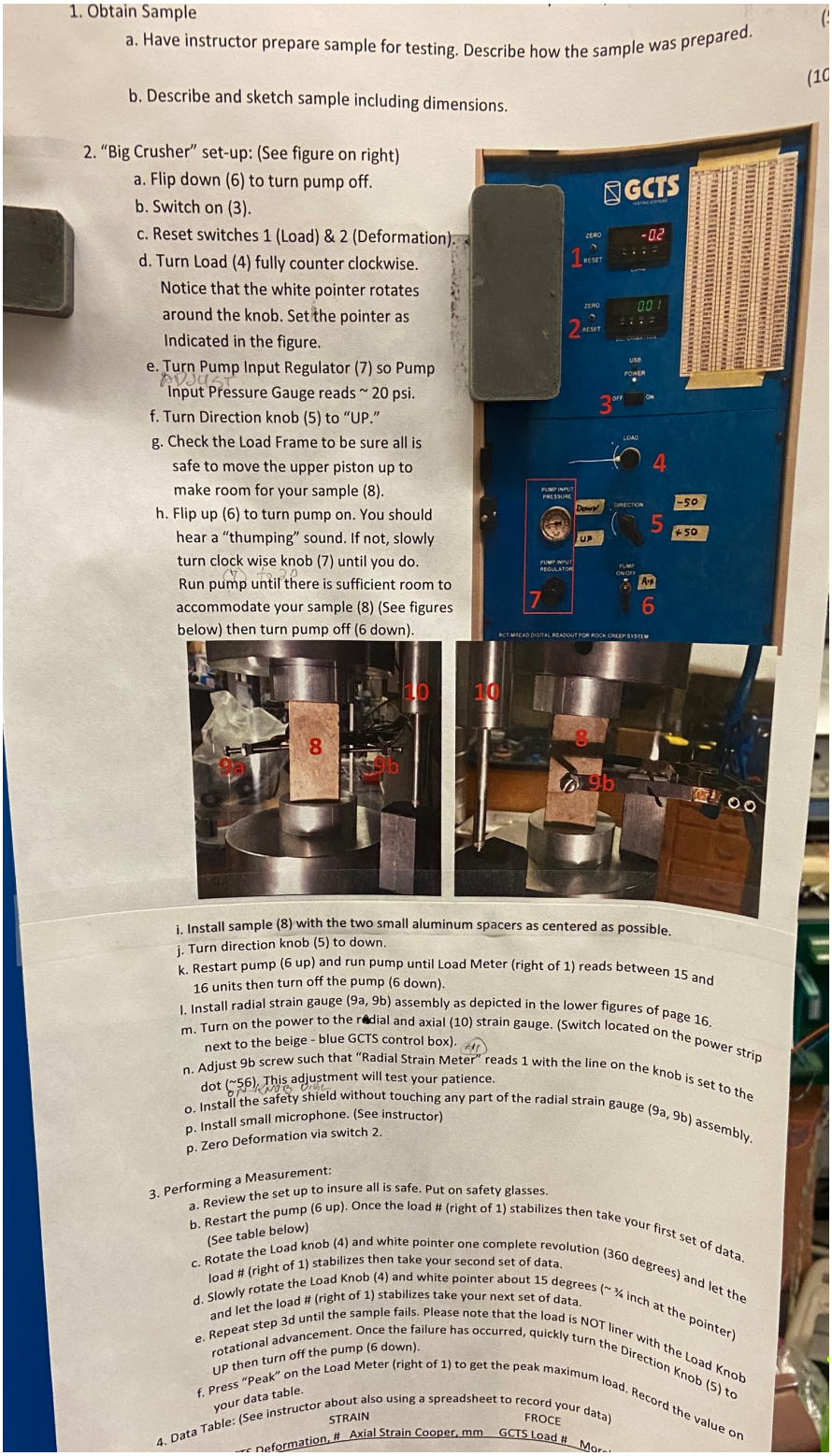

Figure 8: Directions for load cell operation (Enderlin, unpublished).

To calculate the UCS, the maximum load in units of pound force (lbf) is converted to lb in^{-2} using the cross-sectional area of the sample. UCS in lb in^{-2} is then converted to megapascals (MPa) and corrected using the Hoek and Brown (1980) equation. Hoek and Brown (1980) developed an empirical correction based on the heightened probability of flaws present in larger cores. These flaws can lead to lower UCS values not representative of the rock's strength (Hoek and Brown, 1980; Tuncay and Hasancebi, 2009; Tuncay et al., 2019). Conversely, smaller cores likely have larger UCS values because they are less likely to contain flaws (Hoek and Brown, 1980; Tuncay and Hasancebi, 2009; Tuncay et al., 2019). Thus, Hoek and Brown (1980) developed an equation to correct UCS values for cores of different diameters and relate them to 50 mm cores commonly used in engineering (Heap et al., 2018). UCS values can be corrected via:

$$\boldsymbol{\sigma_D = \sigma_{D50}(50/D)^{0.18} \Rightarrow [\sigma_D/(50/D)^{0.18}] = \sigma_{D50},}$$

where σ_d is the UCS for a core sample of a specified diameter, σ_{D50} is the UCS of a core sample with a 50 mm diameter, and "D" is the diameter of the core in question. Going forward, Hoek and Brown (hereafter, H&B) UCS values will be the only values discussed.

Mineralogical Assessment via X-ray Diffraction Analysis

X-ray diffraction was used to determine the bulk mineralogy of the samples. The amount necessary for XRD analysis is approximately two grams (Hauff, 1984), although Omar Harvey (pers. comm.) recommended less powder. Fractured cores from UCS testing were crushed for XRD analysis to link the strength of a sample to its bulk mineralogy. The Rigaku Smartlab SE in the Department of Chemistry & Biochemistry at TCU was used for XRD analysis, and Rietveld refinement was used for mineralogical determinations.

Selecting Samples

30 samples were used for X-Ray diffraction analysis (Table 2). The selection criteria were based on lithology and mechanical strength, sorted first by lithological classification and then by H&B UCS values (low to high). For each lithology one sample with the lowest UCS, one with the highest UCS, and one or two with intermediate values were selected. Hypothetically, mineralogical changes should correlate to mechanical changes.

Table 2: Table shows the various samples given priority for XRD analysis. The scheme used is lithology and UCS. Lithology abbreviations are: CK=chalk, CNGL=conglomerate, LS=limestone, MDRCK=mudrock, NVC=novaculite, SH=shale, SS=sandstone, ST=siltstone.

Sample Name	Median Hardness (HLD)	HB UCS (MPa)	Proposed Primary Lithology	Proposed Secondary Lithology
OKST1-7	700.1	54.23	LS	
TXPK1-1	679.8	117.33	LS	
TXPK1-2	624	82.87	LS	
COT1-5	574.4	47.56	CK	

Sample Name	Median Hardness (HLD)	HB UCS (MPa)	Proposed Primary Lithology	Proposed Secondary Lithology
TXDA1-2	463.3	28.57	LS	CK
TXDA1-3	407.9	17.32	CK	
TXDA1-1	392.6	13.15	LS	CK
OKST1-10	327.3	N/A	MDRCK	
OKST1-9	673.3	37.36	CNGL	
OKST1-15	505.5	36.6	ST	SH
OKST1-1	512.3	57.03	SS	
NMA1-1	762.8	68.94	SS	
NMA1-11	459	25.34	SS	
NMA1-9 Dup.	507.5	18.05	LS	
NMA1-5	599	53.63	CNGL	
OKST1-4	782.5	130.56	LS	
NMA2-1	545.4	45.97	ST	
NMA1-12	381	N/A	MDRCK	
NMA1-15	601.6	73.46	SS	
OKST1-13	295.5	N/A	SH	
NMA1-14	673.8	86.10	SS	
OKST1-18	732.1	44.39	SH	
OKST1-11	496.9	107.05	SH	
COT1-4	367.6	9.22	SS	
COT1-1	604.8	31.55	SS	
TXBB1-1	941.8	215.79	NVC	
TXBB1-2	923.9	65.31	NVC	
OKST1-14	887.3	307.8	SH	
OKST1-12	752.5	77.33	SH	
COT1-6	566	26.68	ST	

Powdering Samples

To properly prepare samples for XRD analysis, samples were crushed into a fine powder using an automated mortar and pestle (Figure 9). The machine uses a steel cylindrical container with two steel balls to crush each sample (Figure 9, bottom). The machine operated for two minutes per sample. Once the powdering process was

complete, 0.4 grams of the sample were placed in a plastic test tube and the excess powder in labeled sample bags.

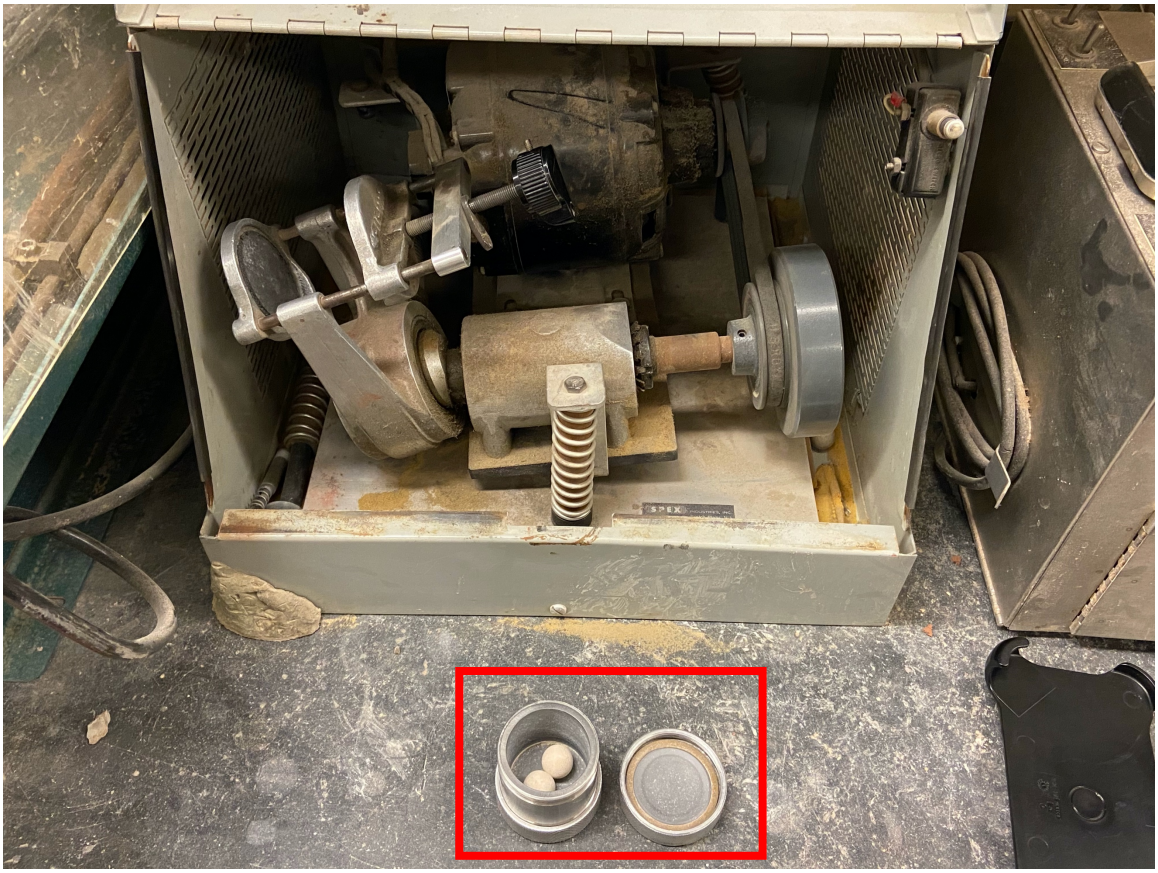

Figure 9: Picture shows the automated mortar and pestle used to powder samples for XRD analyses. The red box highlights the metal sample holder**.**

XRD Scanning

A Rigaku Smartlab SE in the Department of Chemistry & Biochemistry at TCU was used to scan the samples. Samples were loaded into a 0.5 mm deep, square cavity, microscope slide. The surface of the powder was kept as flat as possible and no powder was spilled outside of the cavity. Slides were loaded into the machine, which was set to 40kV with a 2-theta scan range of 5-50 degrees. The scan duration for each sample was

approximately 12.5 minutes. Once scanned, sample data was downloaded in both RASX and CSV file formats and the CSV files was used during Rietveld refinement.

Rietveld Refinement

The Match program was used to determine the mineralogy of each specimen based on the CSV file from the XRD scans. The raw data was smoothed and mineral phases were added as recommended by the program. Rietveld refinement in the program was used to add or subtract mineral phases until the program returned a reasonable value for both the Bragg R and Chi-squared values. Important statistics and weight percent of each mineral phase were exported for future analyses.

XRD Data

Mineralogical data were plotted on a ternary diagram, allowing for better visualization of the relationship between each sample's mineralogy and mechanical properties. The bins are silicate minerals (quartz and feldspars), carbonate minerals (calcite and dolomite), and clay minerals (clays and micas). Mineralogical and mechanical data (hardness and strength) were plotted for each sample in OriginPro.

Statistical Analyses

Several statistical analyses were conducted in Past4 (Hammer et al., 2001). First, normality tests for steel block calibration data were completed. Based on these results (Appendix 1) non-parametric statistics were used for sample characterization (Aoki and Matsukura, 2008; Wilhelm et al., 2016; Colwell, 2018). Specifically, Spearman's Rank Order Correlation (SROC) was used when comparing datasets because it can be used with both parametric and non-parametric data. Other statistical analyses included Multiple Linear Regression and Principal Components Analysis (Grima and Babuska,

1999; Meulenkamp and Grima, 1999; Kahraman, 2001; Tiryaki, 2008). These statistical methods were compared to each other to compare effectiveness with the data.

Graphical Analyses

Graphical representations of the data made in Microsoft Excel, OriginPro, and Past4 (Hammer et al., 2001) allow better visualizations of the relation between datasets. Data are depicted based on field lithologic classification. Thus, trends and natural variations in data become apparent.

Spearman's Rank-Order Correlation (SROC)

SROC is the non-parametric version of the Pearson's Product-Moment correlation coefficient R, which is used to determine which variables have statistically significant relationships and the nature of these relationships. The null hypothesis for this method states that the relationship between datasets is random. The alternative hypothesis is that the relationship between two datasets is not random with an alpha-level of 0.05 to be statistically significant. SROC compares the median of a dataset against other medians. Thus, it is suited for most of the data, which is non-parametric. Also, this statistical method can be used on parametric datasets, thus enhancing its utility.

Principal Component Analysis (PCA)

PCA is an exploratory method that combines independent variables to better find natural groups within datasets, thus allowing the development of better predictive models (Tiryaki, 2008). Since multiple datasets were used for each sample, eliminating the non-essential variables helped determine the most important variables. This homogenous dataset was then used to draw conclusions about the data (Tiryaki, 2008). Therefore, for

this project, where multiple datasets are compiled, a statistical method to reduce the number of these variables was necessary.

Multiple Linear Regression

After analyzing the data using SROC and PCA, an equation was derived using Multiple Linear Regression (MLR) to relate hardness to its controlling factors. Meulenkamp and Grima (1999) used multiple linear regression in conjunction with fuzzy logic software, but their study did not account for bulk mineralogy. In this study an attempt was made to derive an equation that accounts for bulk mineralogy and other physical properties. Additionally, it helps to determine if accurate equations can be developed without fuzzy logic.

To develop an equation, the linear model function in Past4 (Hammer et al., 2001) was used. The independent variables considered for mechanical hardness were: total silicates, total carbonates, total clays, density, effective porosity, and sample volume.

Using the initial variables, Past4 calculates the model allowing examination of the p-value for each independent variable. Variables with high p-values (p-value > 0.05) are manually eliminated from consideration because Past4 does not automate this process. After a variable is eliminated, the calculation is run again; this process continues until each independent variable has a p-value less than 0.05. At this point the remaining variables and their coefficients are incorporated into a linear regression equation.

Measured versus Predicted Values

After MLR of hardness, an equation predicting UCS from hardness was derived. If hardness is a good predictor of UCS, the Root Mean Square Error (RMSE) of predicted UCS will be normally distributed. The measured hardness and UCS for 28 samples were

randomly selected as a calibration dataset, and used to derive a best-fit line. The equation of this line was then used to predict UCS for the remaining 20 samples. The RMSE was calculated for the 20 samples. Every five iterations, normality was tested for both the coefficients of the best-fit equation, and the RMSE. A general equation relating hardness to UCS was then derived from the mean values of these coefficients.

Chapter 3: Results

Mechanical Hardness

Mechanical hardness was tested in stages. First, a viable sample holder was determined from six possible options; results from this are summarized in Appendix 1. Then, rock samples were tested prior to and after oven drying to determine if any changes occurred. During this procedure the changes in mass were also recorded.

Testing Sample Holders

The hardness data for the various sample holders was analyzed using normality tests and descriptive statistics. Because a majority of the sample holders yielded non-normal data (Table 3), median values are used. Based on the results, the two best methods of securing samples are the vise and tabletop (Table 3), as both have mean and median values in the acceptable range given by ASTM-A956 (Table 3). The only other method to consider is the table clamped method. However, this method is unwieldy and does not offer better results than either the tabletop or vise.

Table 3: Statistics from testing various sample holders**.**

Statistics	Tabletop	Vise	Sandbox	Table Clamped	Table w/1 layer cardboard	Wood block
Number	20	20	20	20	20	20
Mean	769.9	770.8	782.7	771.1	777.3	786.1
Median	772	770	777	770	776.5	781
Shapiro-Wilk W	0.82	0.93	0.60	0.92	0.86	0.40
p(normal)	$1.9*10^{-3}$	0.19	$3.04*10^{-06}$	0.10	$7.4*10^{-3}$	$4.81*10^{-08}$

Table Top vs. Vise 200 Impacts Test Results

After obtaining initial sample holder results, both the tabletop and vise methods were re-tested to better understand the calibration block data, to determine if the data distribution became more normal with more measurements, and to check the accuracy of each holder with more data.

None of the re-testing resulted in normally distributed data (Figure 10). Thus, median values were used with the nonparametric Wilcoxon test to compare the medians of the re-test data with the engraved block value. The vise and tabletop median values are statistically the same as the Side B value of 769 HLD (Figure 10; Table 4). However, this is not the case for the vise, tabletop, and Side A value (Figure 10). Therefore, Side B of the steel block was used in future calibration checks. Both holders suffice statistically, but the vise was used because it allowed leveling of samples prior to testing.

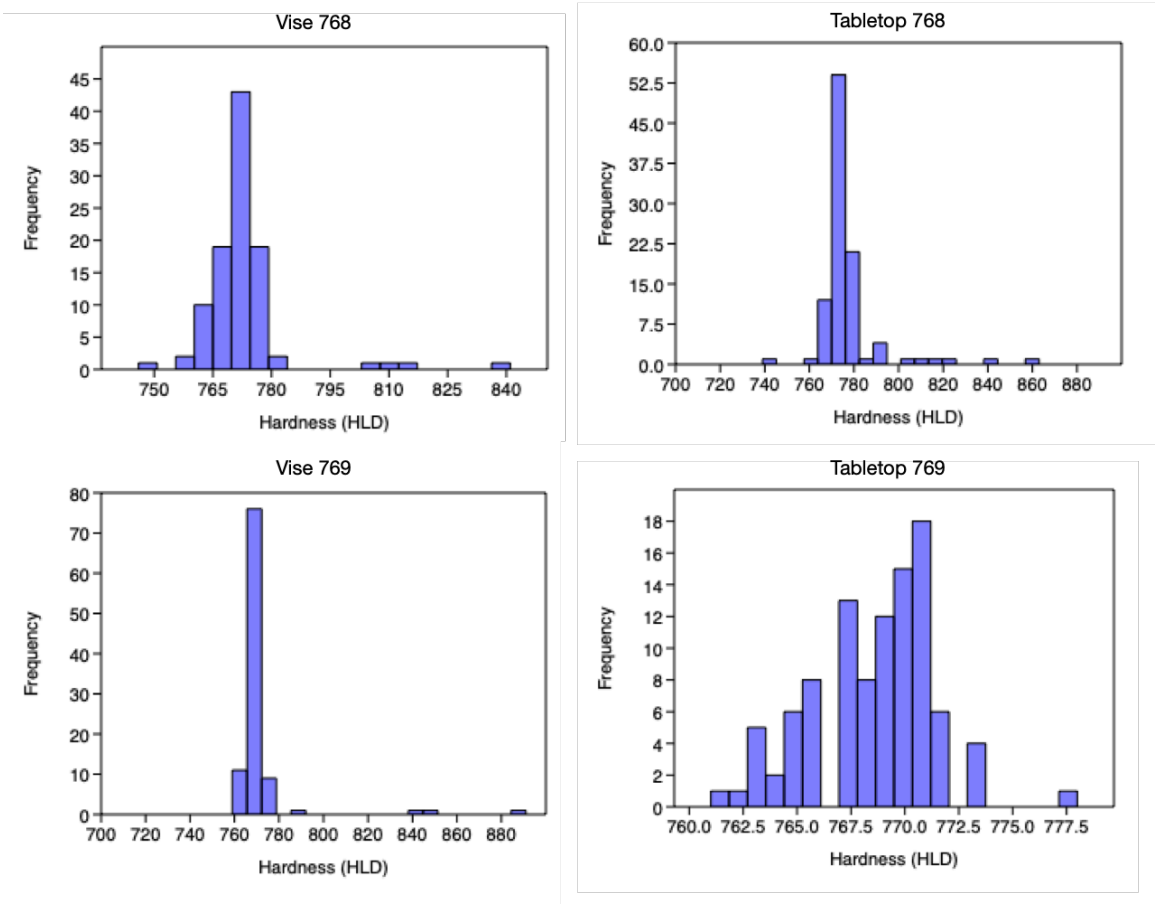

Figure 10: Histograms of the four calibration re-tests**.** Each graph visually shows the distribution of calibration data. Vise 768 (upper left) and Tabletop 768 (upper right) display the distribution of calibration data for the Side A re-tests of the vise and tabletop mounts, respectively. Vise 769 (lower left) and Tabletop 769 (lower right) show calibration data for the Side B tabletop re-tests of the vise and tabletop mounts, respectively.

Table 4: Statistics for the sample holder re-tests**.**

	Vise 768	**Vise 769**	**Tabletop 768**	**Tabletop 769**
Number	100	100	100	100
Mean	772.47	771.93	777.05	768.57
Median	771	770	774	769
Shapiro-Wilk W	0.65	0.34	0.61	0.96
Probability (normal)	4.32×10^{-14}	3.70×10^{-19}	6.26×10^{-15}	7.5×10^{-3}
Given value	768	769	768	769
Sample median:	771	770	774	769
Probability (same median):	4.35×10^{-07}	0.37	2.32×10^{-15}	0.17

Pre-Dry vs Post-Dry Testing

After initial hardness testing, samples were dried at 80°C for 120 hours and subsequently the hardness of each sample was remeasured to determine the effect moisture content has on hardness.

Water Mass Lost

Drying led to a decrease in mass for 31% of the samples. These included five limestones, three silty shales, two sandstones, two conglomerates, one mudrock, one shale, and one chalk (Figure 11). The greatest mass reduction occurred in NMA1-3, which is shale (Figure 11). Novaculites as a group, experienced no mass change (Figure 11). Similarly, most groups contained numerous samples that experienced no mass change, explaining the wide bases of the violin plots, and lack of median line (black line) on the interior boxplot (Figure 11).

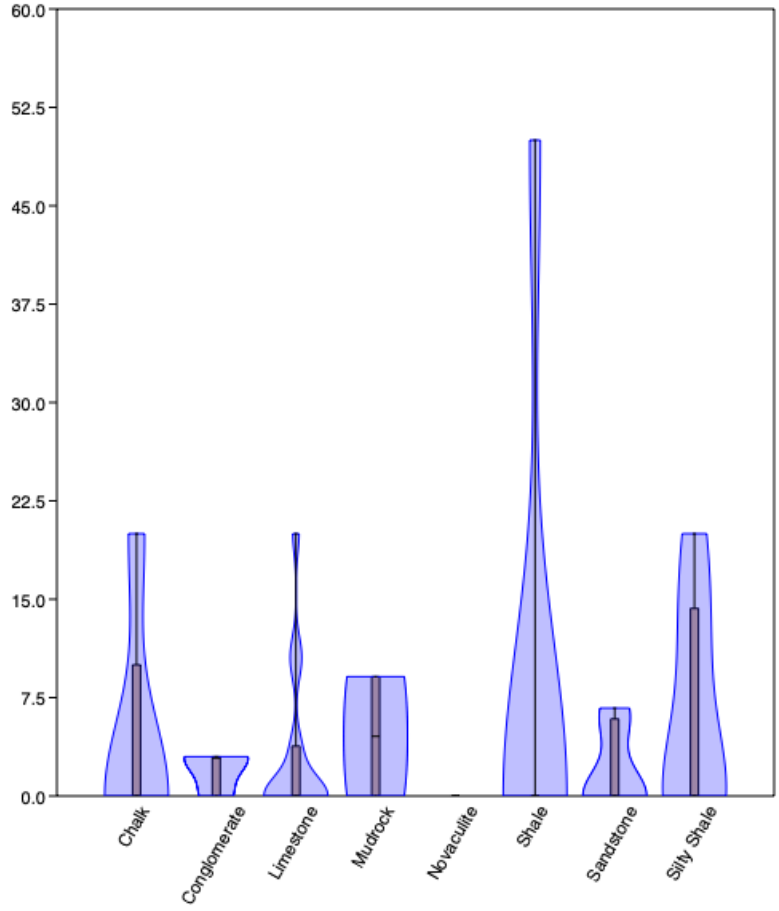

Figure 11: Percent mass change by lithology as a result of drying**.**

Hardness Results

Hardness changed between the oven dried samples and their unaltered counterparts (Figure 12). Perpendicular hardness increased in 78% of samples after drying, whereas parallel hardness increased in 76% of samples (Figure 12). The largest increase perpendicular to bedding occurred in OKST1-12 (Figure 12) whose weathering rind was only recognized and trimmed after drying.

Novaculites as a group have the highest median hardness, whereas mudrocks have the lowest (Figure 13). The median hardness for conglomerate and limestone is similar,

as is the median hardness for shale and sandstone (Figure 13). Most groups (conglomerate, limestone, shale, and sandstone) have a median hardness between 500 and 700 HLD (Figure 13). Shales have the largest range of hardness, whereas novaculites have the smallest (Figure 13). It is unclear if the variation in hardness occurs due to intrinsic properties, or due to the number of samples in each group. For instance, there are 14 limestone samples, but only two mudrock samples (Figure 13). Therefore, limestone hardness might be better represented simply because there are more limestones than mudrocks or other lithologies. Regardless, this does not invalidate the trends that exist in the data.

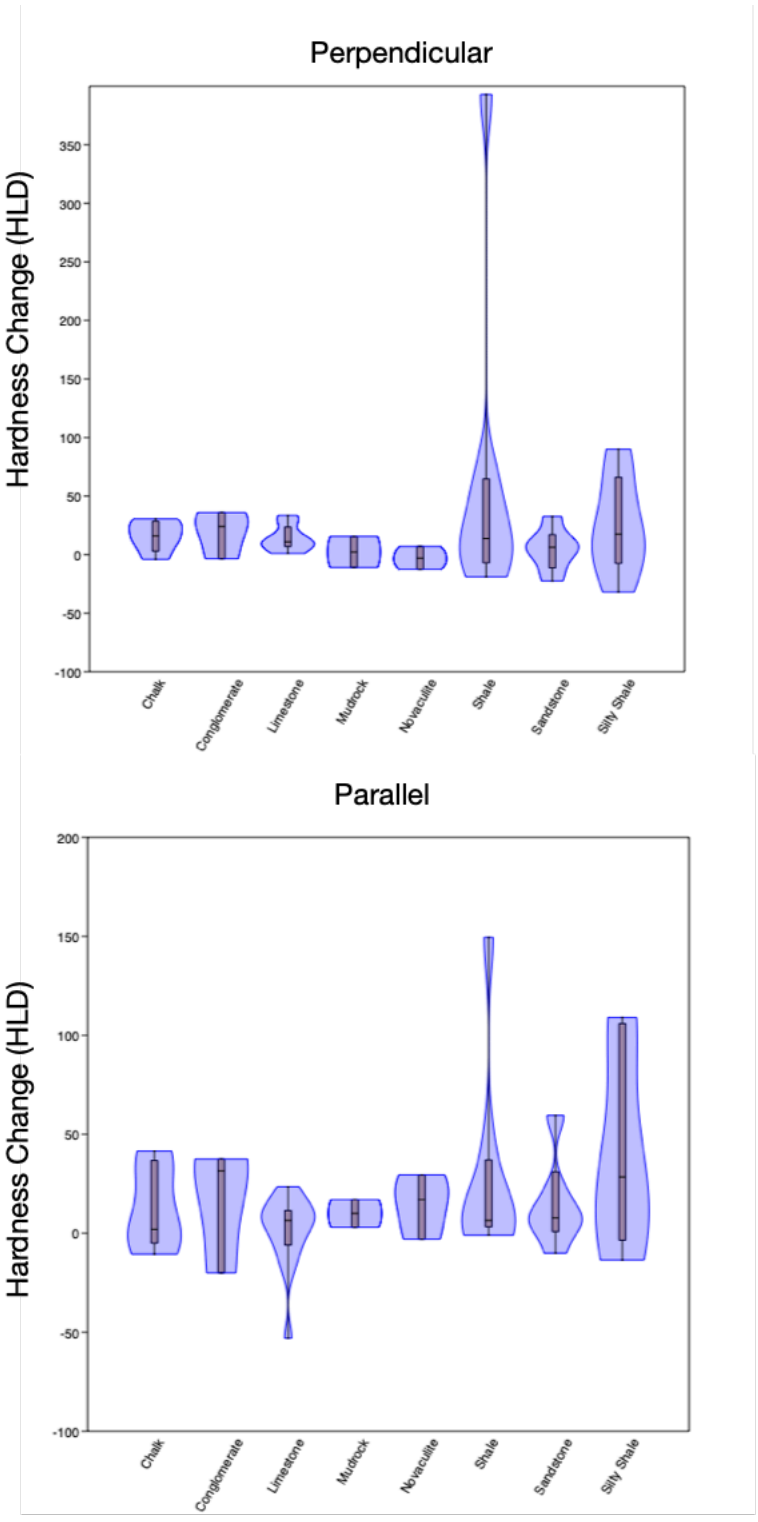

Figure 12: Changes in hardness by lithology and sampling orientation relative to bedding due to drying.

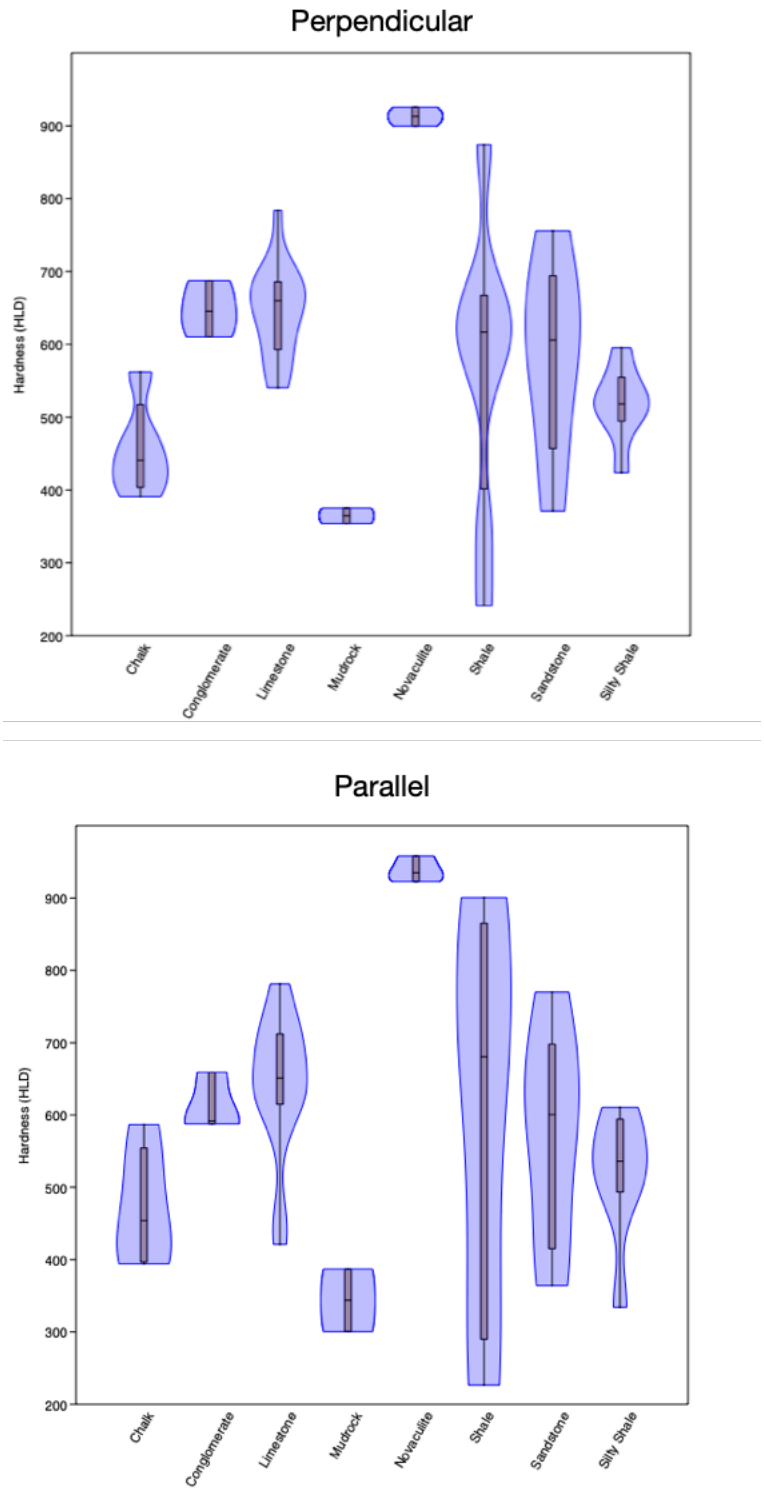

Figure 13: Average median hardness by lithology and sampling orientation relative to bedding.

Anisotropy

By lithology, variations exist in median anisotropy and corresponding interquartile range (Figure 14). The aggregate median anisotropy for all samples is 1 and the interquartile range is 0.08 (see Appendix 2 for complete statistical data). Shales have the lowest median anisotropy at 0.94 with an interquartile range of 0.305 (Figure 14). The largest median anisotropy 1.075 belongs to mudrocks followed by conglomerates at 1.04 (Figure 14). The interquartile range for mudrocks is 0.21, and 0.05 for conglomerate (Appendix 2). The deviation in median anisotropy for these groups from the aggregate is: 6% (shale), 7.5% (mudrock), and 4% (conglomerate). Median anisotropy for other groups is: 0.99 (limestone), 0.98 (novaculite), 1.01 (sandstone), and 1.02 (silty shale) (Figure 14). Thus, these other groups all have median values within 2% of the aggregate median. The interquartile range for the remaining groups is <0.10, except for silty shale (0.16). Thus, these samples are not only more isotropic than shales, conglomerates, or mudrocks, but they also have a tighter distribution of values around their medians.

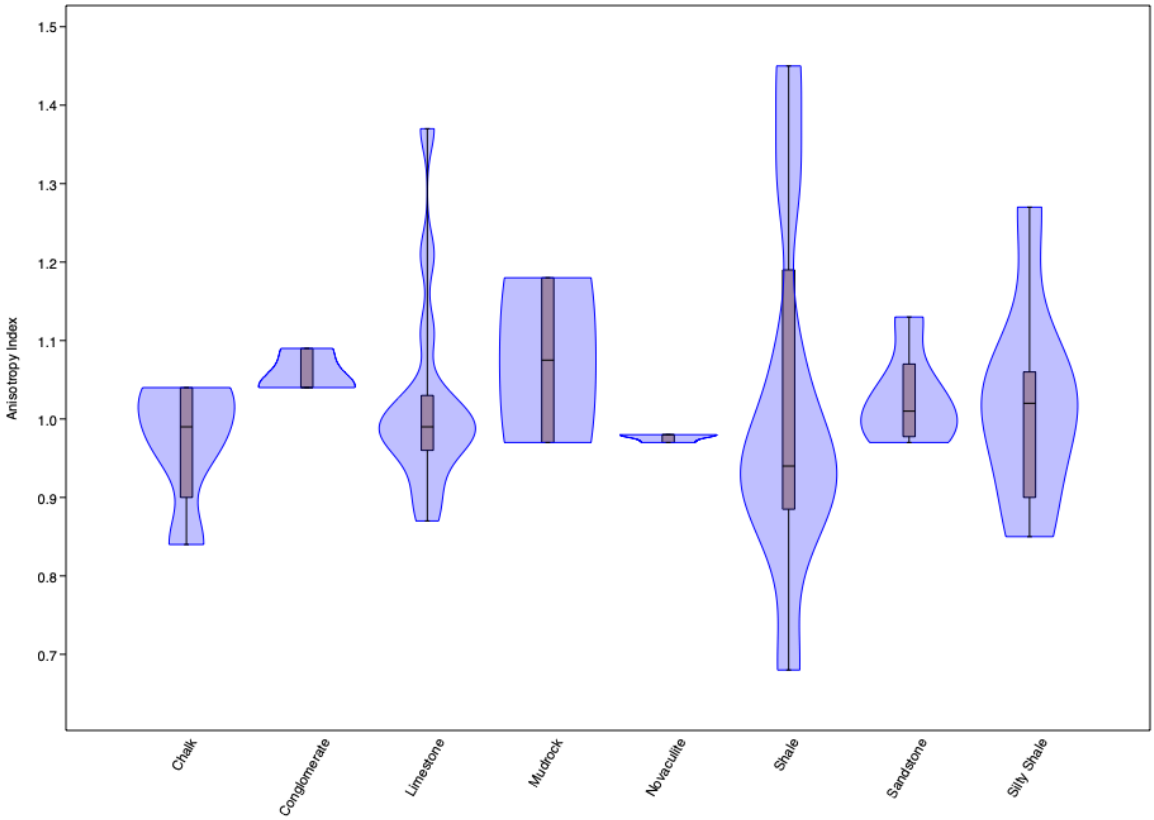

Figure 14: Hardness anistropy by lithology**.**

Coring

Number of Samples Cored

Of the 48 samples, six were too friable for core drilling. These samples included: NMA1-2, NMA1-3, NMA1-7, NMA1-12, OKST1-10, and OKST1-13. Attempts to drill cores or cut rectangular prisms were unsuccessful as samples simply disaggregated. These six samples were either fine-grained silty shales (NMA1-2; NMA1-7), shales (NMA1-3; OKST1-13), or mudrocks (NMA1-12; OKST1-10). Samples cut as rectangular plugs for load cell testing included: OKST1-3, OKST1-6, OKST1-8, OKST1-15, OKST1-17, OKST1-18, and TXDA1-3. The lithologies of these rocks are: limestone (OKST1-3 and OKST1-8), chalk (OKST1-6 and TXDA1-3), and shale (OKST1-15, OKST1-17, and OKST1-18). Due to its high hardness, only one core was recovered from TXBB1-1, even after changing various drilling parameters (RPM, weight on bit).

Density Results

Sample density varies from 1.66 g/cm^3 up to 3.36 g/cm^3 (Figure 15). TXPK1-2 has the highest density sample at 3.36 g/cm^3, and is a limestone (Figure 15). It is unknown what caused the high density for TXPK1-2. The lowest density sample is a shale (OKST1-11) at 1.66 g/cm^3 (Figure 15). Densities between 2.19 g/cm^3 and 2.58 g/cm^3 account for 50% of all values (Figure 15). By lithology, density ranges are: 1.83-2.45 g/cm^3 (chalk), 2.45-3.06 g/cm^3 (conglomerate), 2.27-3.36 g/cm^3 (limestone), 1.71-2.86 g/cm^3 (mudrock), 2.36-2.73 g/cm^3 (novaculite), 1.66-2.62 g/cm^3 (shale), 1.84-2.85 g/cm^3 (sandstone), and 2.14-2.56 g/cm^3 (silty shale) (Figure 15). All rocks were found along road cuts exposed to weathering, potentially leading to densities lower than normal due to dissolution of cement or grains.

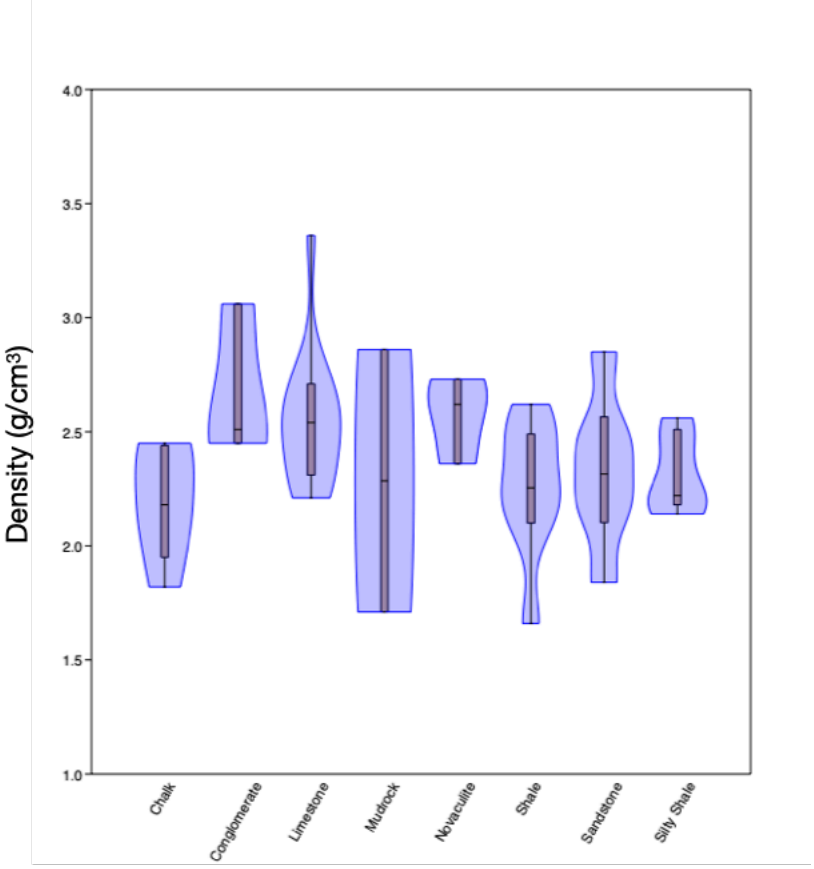

Figure 15: Sample density by lithology**.**

Sample Volume Results

Using the density and mass of each sample, the whole rock volume was calculated and categorized by lithology (Figure 16). The sample with the largest volume is NMA1-16 (Figure 16). Five samples have a volume less than 197 cm^3 (Figure 16) including sample OKST1-17, which broke in the lab. Sample volume is not an intrinsic property to a rock because each sample was cut to a desired volume, unlike other properties such as porosity, which could not be controlled. Thus, these data are only shown because they are used in future analyses.

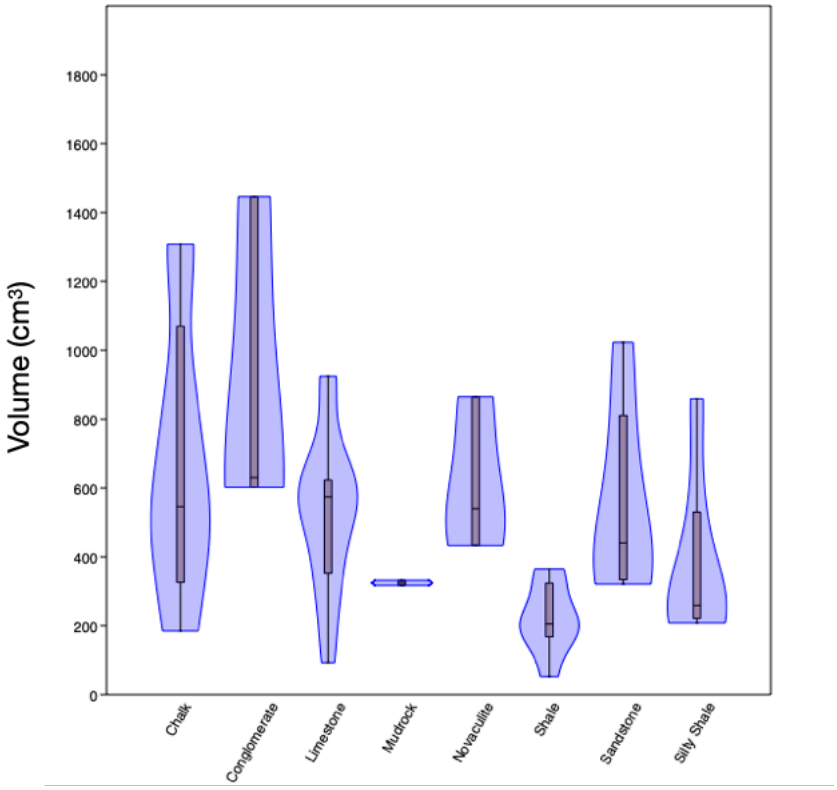

Figure 16: Sample volume by lithology**.**

Effective Porosity Results

Effective porosity was calculated for all samples (Figure 17). The sample with the lowest effective porosity is OKST1-2, which is a limestone (0.20%, Figure 17). The sample with the highest effective porosity is TXDA1-1, which is a chalk (29.00%, Figure 17). By lithology, effective porosity ranges from 4.5-29.0% (chalk), 2.0-3.7% (conglomerate), 0.2-22.3% (limestone), 6.7-23.1% (mudrock), 1.5-5.0% (novaculite), 4.5-22.0% (shale), 1.2-23.0% (sandstone), and 4.6-24.4% (silty shale) (Figure 17).

Effective porosity was measured in all samples, including novaculites and shales. Being able to obtain these data suggests that the water immersion porosimetry method used is valid and the role of effective porosity on the mechanical behavior is testable.

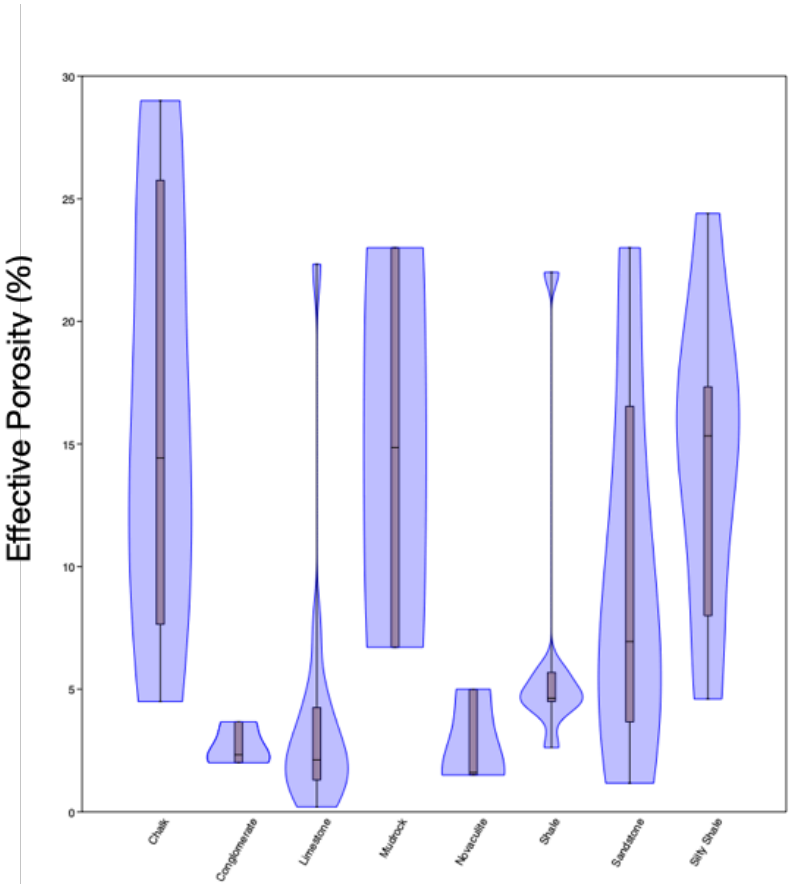

Figure 17: Effective porosity results by lithology**.**

Unconfined Compressive Strength

After the maximum load was measured for each sample, the UCS was calculated. The strongest sample is OKST1-14, which is shale (Figure 18). Rocks that could not be cored (mudrocks), are not plotted. Novaculites, as a group, are the strongest rocks, whereas most other groups have overlapping UCS values (Figure 18). By lithology, each group's median UCS is: 28.6 MPa (chalk), 48.6 MPa (conglomerate), 59.9 MPa (limestone), N/A (mudrock), 94.9 MPa (novaculite), 75.2 MPa (shale), 50.3 MPa (sandstone), and 46.0 MPa (silty shale) (Figure 18).

Post-dry hardness correlates positively to UCS, and the relationship between the two is a power relationship (Figure 19). The R^2-values for perpendicular hardness and

UCS, and parallel hardness and UCS are 0.49 and 0.41, respectively (Figure 19). Therefore, perpendicular hardness correlates better to UCS than parallel hardness (Figure 19). Because UCS was measured perpendicular to bedding, it is reasonable that perpendicular hardness has a higher R^2-value than parallel hardness.

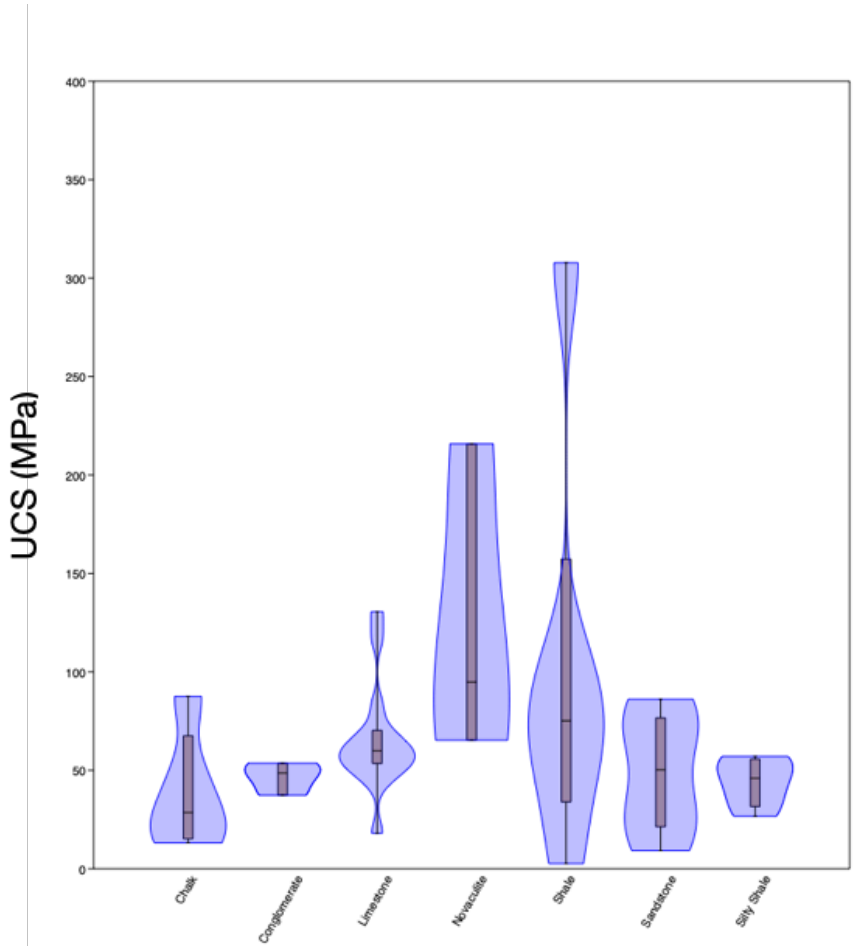

Figure 18: H&B UCS values by lithology**.**

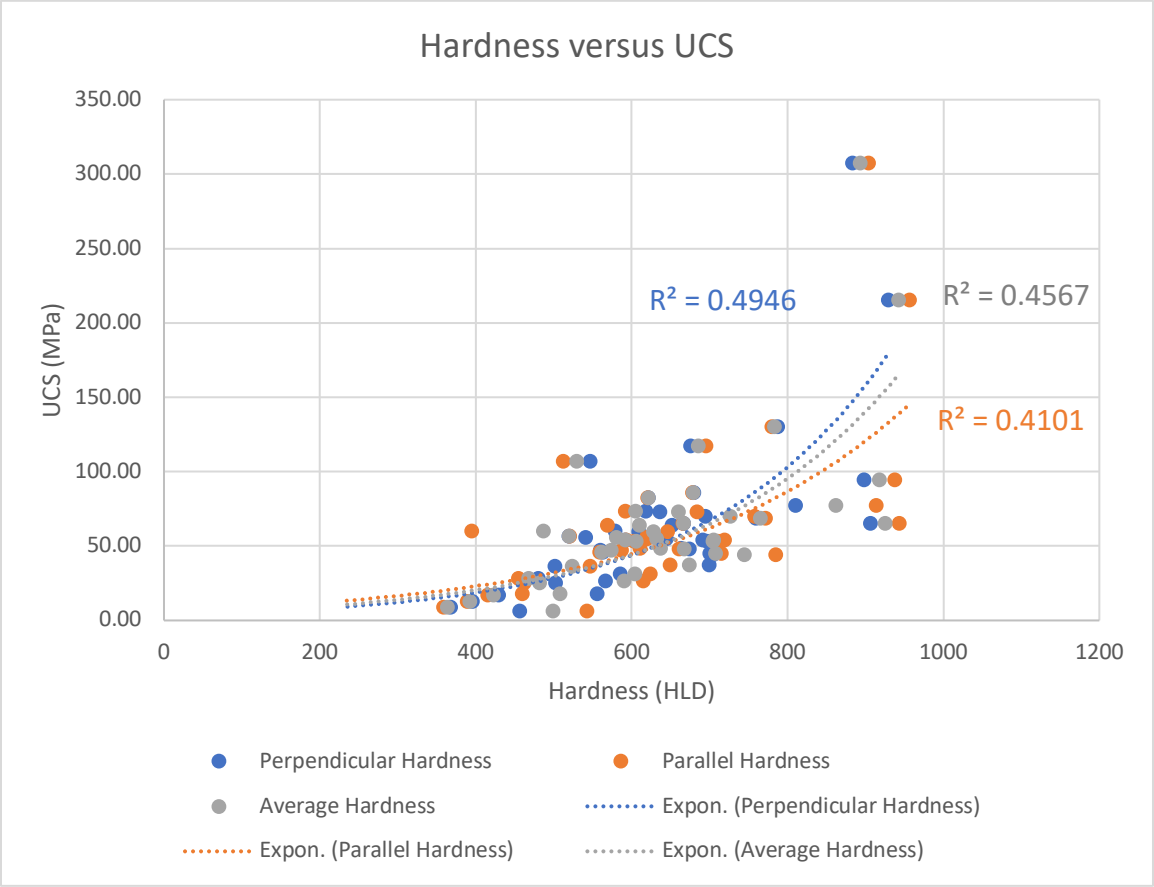

Figure 19: Relationship between perpendicular hardness, parallel hardness, average hardness, and UCS using Hoek and Brown (1980) correction.

XRD Results

XRD data are shown on a ternary diagram with mechanical hardness and UCS plotted as Z-values (Figure 20). Bubble size indicates mechanical hardness values, whereas colors indicate UCS values. Many samples plot along either the "Total Carbonate/Quartz + Feldspar" or "Total Clay/Quartz + Feldspar" axes, and only three samples contain all three mineralogical components in some quantity. Three samples (OKST1-10; NMA1-12; OKST1-13) that could not be tested (light blue; Figure 20) in the load cell have the lowest median hardness values (Table 5). Generally, greater mechanical hardness and strength trend toward higher silica or carbonate content (Figure

20). Some discrepancies exist, particularly in the purple circles (OKST1-11; NMA1-14; NMA1-15) at the bottom of Figure 20. Despite having higher clay content than other samples, these three samples have higher hardness and UCS values than other samples containing 100% silicate or carbonate minerals (Figure 20). Theoretically, the presence of clay should lead to lower mechanical values. Thus, it is likely other factors affect mechanical parameters than just mineralogy alone.

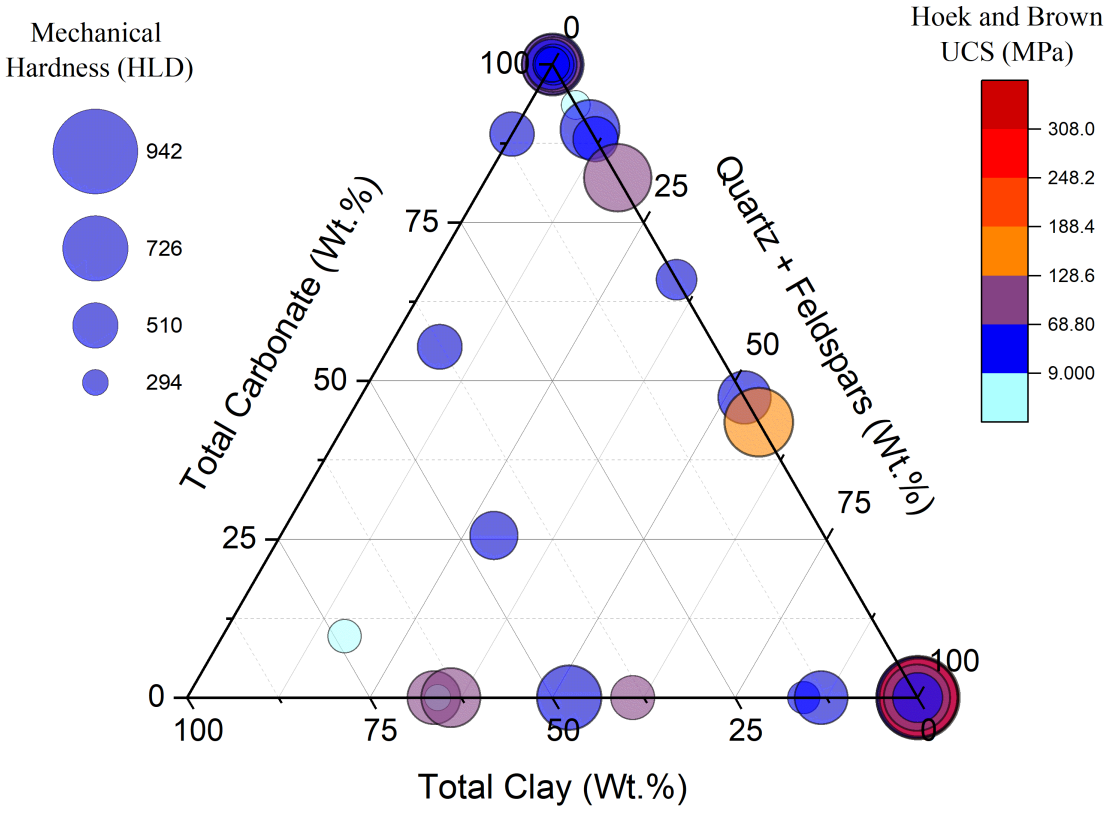

Figure 20: XRD ternary diagram showing mechanical hardness and UCS. Larger bubbles indicate a larger average median hardness for a sample. UCS values are color coded**.**

Table 5: Bulk mineralogy and mechanical properties of the samples analyzed with XRD**.**

Sample Name	Total Carbonate (wt.%)	Total Clay (wt.%)	Quartz + Feldspars (wt.%)	Median Hardness (HLD)	HB UCS (MPa)
OKST1-7	100	0	0	700.1	54.23
TXPK1-1	100	0	0	679.8	117.33
TXPK1-2	100	0	0	624	82.87
COT1-5	100	0	0	574.4	47.56
TXDA1-2	100	0	0	463.3	28.57
TXDA1-3	100	0	0	407.9	17.32
TXDA1-1	100	0	0	392.6	13.15
OKST1-10	93.6	0	6.4	327.3	N/A
OKST1-9	89.7	0	10.3	673.3	37.36
OKST1-15	89	11	0	505.5	36.6
OKST1-1	88.2	0	11.8	512.3	57.03
NMA1-1	82.1	0	17.9	762.8	68.94
NMA1-11	66	0	34	459	25.34
NMA1-9 Dup.	55.4	37.7	6.9	507.5	18.05
NMA1-5	47.4	0	52.6	599	53.63
OKST1-4	43.5	0	56.5	782.5	130.56
NMA2-1	25.6	45.2	29.2	545.4	45.97
NMA1-12	9.7	73.5	16.7	381	N/A
NMA1-15	0	66.2	33.8	601.6	73.46
OKST1-13	0	65.7	34.3	295.5	N/A
NMA1-14	0	63.9	36.1	673.8	86.10
OKST1-18	0	47.7	52.3	732.1	44.39
OKST1-11	0	39	61	496.9	107.05
COT1-4	0	15.6	84.4	367.6	9.22
COT1-1	0	13.2	86.8	604.8	31.55
TXBB1-1	0	0	100	941.8	215.79
TXBB1-2	0	0	100	923.9	65.31
OKST1-14	0	0	100	887.3	307.8
OKST1-12	0	0	100	752.5	77.33
COT1-6	0	0	100	566	26.68

Statistical Analyses

The statistical analyses used in this study are Spearman's Rank-Order Correlation (SROC), Principal Components Analysis (PCA), and Multiple Linear Regression (MLR). The techniques are described in the Methods section above.

SROC

Data used for SROC were broken into two groups: physical data for all samples (Table 6), and physical data including mineralogy (Table 7).

Multiple relationships arise between mechanical properties and other variables. Average median hardness has statistically significant relationships to: H&B UCS, density, effective porosity, and anisotropy, but not sample volume (Table 6). H&B UCS has statistically significant relationships to: density, water mass loss, and effective porosity (Table 6). Density has a statistically significant relationship with effective porosity, whereas effective porosity has a statistically significant relationship with sample volume (Table 6).

Relationships exist between the mineralogical data and physical data (Table 7). First, total carbonate has statistically significant relationships to total clay, quartz+feldspars, and sample volume (Table 7). Quartz+feldspars have a statistically significant relationship with average median hardness, which is the only similar mineralogical relationship (Table 7). All other relationships are physical, such as those described above in Table 6. However, some differences exist between these two analyses (Table 6 and Table 7). For example, H&B UCS is related to density in Table 6, but not Table 7. Also, effective porosity and sample volume do not have a statistically significant

relationship in Table 7. Relationship discrepancies between Table 6 and Table 7 could result from dataset size used in SROC (48 versus 30, respectively).

Table 6: Spearman's rank correlation for all mechanical and independent properties. Calculated statistics are given at the bottom, whereas the probability is given at the top of the chart.

		Probability									
		Average Median Pre-Dry Hardness (HLD)	Average Median Post-Dry Hardness (HLD)	Average Median Hardness (HLD)	H&B UCS Correction (MPa)	Density (g/cc)	Effective Porosity	Volume (cc)	Pre Dry Hardness Anisotropy Index	Post Dry Hardness Anisotropy Index	% Mass Change from Water Loss
Statistic	Average Median Pre-Dry Hardness (HLD)		3.5x10^-34	2.1x10^-40	1.4x10^-4	4.6x10^-3	3.8x10^-5	1.3x10^-1	8.4x10^-4	6.1x10^-3	3.8x10^-1
	Average Median Post-Dry Hardness (HLD)	0.98		2.0x10^-50	5.8x10^-5	3.5x10^-3	6.2x10^-5	2.2x10^-1	2.7x10^-4	2.1x10^-3	3.5x10^-1
	Average Median Hardness (HLD)	0.99	1.00		6.7x10^-5	3.2x10^-3	6.3x10^-5	1.7x10^-1	2.8x10^-4	2.6x10^-3	3.5x10^-1
	H&B UCS Correction (MPa)	0.55	0.58	0.58		4.0x10^-2	9.6x10^-3	4.1x10^-1	5.4x10^-2	1.3x10^-1	4.8x10^-2
	Density (g/cc)	0.40	0.41	0.42	0.32		4.7x10^-4	4.4x10^-1	8.8x10^-2	9.5x10^-1	4.4x10^-1
	Effective Porosity	-0.56	-0.54	-0.54	-0.40	-0.49		3.3x10^-2	2.8x10^-1	8.8x10^-1	1.0x10^-1
	Volume (cc)	0.22	0.18	0.20	-0.13	0.11	-0.31		3.9x10^-1	2.5x10^-1	1.5x10^-1
	Pre Dry Hardness Anisotropy Index	-0.47	-0.50	-0.50	-0.30	-0.25	0.16	0.13		1.2x10^-12	2.1x10^-1
	Post Dry Hardness Anisotropy Index	-0.39	-0.43	-0.42	-0.24	0.01	0.02	0.17	0.82		4.3x10^-1
	% Mass Change from Water Loss	-0.13	-0.14	-0.14	-0.31	-0.11	0.24	-0.21	0.18	0.11	

Table 7: Spearman's rank correlation for all samples used for XRD analysis. Calculated statistics are given at the bottom, whereas the probability is given at the top of the chart**.**

		Probability										
		Total Carbonate (wt.%)	Total Clay (wt.%)	Quartz + Feldspars (wt.%)	Average Median Hardness (HLD)	HB UCS (MPa)	Density (g/cc)	Effective Porosity	Sample Volume (cc)	Pre-Dry Anisotropy Index	Post-Dry Anisotropy Index	% Mass Change from Water Loss
Statistic	Total Carbonate (wt.%)		3.6x10^-3	5.9x10^-12	0.22	0.20	0.79	0.49	0.05	0.64	0.95	0.37
	Total Clay (wt.%)	-0.51		0.48	0.10	0.67	0.97	0.74	0.57	0.08	0.18	0.38
	Quartz + Feldspars (wt.%)	-0.91	0.13		0.04	0.13	0.88	0.32	0.06	0.92	0.58	0.49
	Average Median Hardness (HLD)	-0.23	-0.31	0.39		7.13E-06	0.03	0.02	0.92	0.00	0.00	0.24
	HB UCS (MPa)	-0.26	-0.09	0.30	0.75		0.15	0.03	0.07	0.33	0.36	0.15
	Density (g/cc)	0.05	-0.01	-0.03	0.39	0.29		0.01	0.46	0.01	0.44	0.88
	Effective Porosity	0.13	0.06	-0.19	-0.42	-0.43	-0.46		0.34	0.67	0.60	0.10
	Sample Volume (cc)	0.37	-0.11	-0.35	-0.02	-0.35	0.14	-0.18		0.95	0.86	0.07
	Pre-Dry Anisotropy Index	-0.09	0.32	-0.02	-0.54	-0.20	-0.46	0.08	-0.01		9.5x10^-6	0.88
	Post-Dry Anisotropy Index	0.01	0.25	-0.11	-0.57	-0.18	-0.15	-0.10	0.03	0.71		0.85
	% Mass Change from Water Loss	0.17	-0.17	-0.13	-0.22	-0.28	-0.03	0.30	-0.34	-0.03	0.04	

PCA

PCA was used in an attempt to determine previously undetected associations between the data. However, the best results only returned group relationships seen elsewhere (Figure 21). For example, PCA shows that UCS varied within groups of the same mineralogy as shown in Figure 20. In addition, hardness also varied between samples of the same mineralogy in both PCA (Figure 21) and on the ternary diagram (Figure 20). Therefore, while useful, PCA only reinforced associations found with other measures in this study.

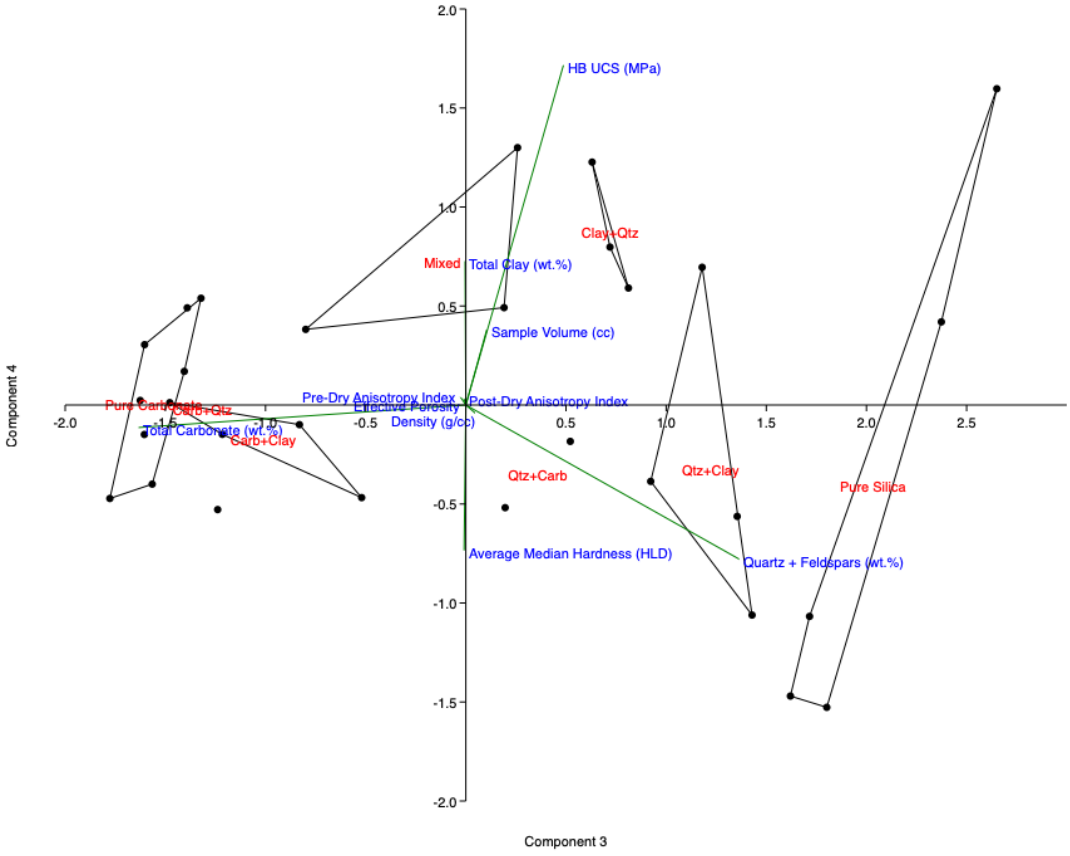

Figure 21: Principal components analysis showing PC3 vs PC4 for the subset of data containing XRD values and other properties.

MLR of Hardness

The variables controlling mechanical hardness are total carbonate, total silicates, and density (Table 8). Using the results (Table 8), the following equation shows factors governing Leeb hardness of a rock based on: carbonate content (Wt. %), silicate content (Wt. %), and density (g/cm^3):

$$HLD = -141.01 + 2.05Carb._{wt\%} + 4.58Sil._{wt\%} + 198.80\rho,$$

where Carb.$_{wt\%}$ is total carbonate (calcite and dolomite), Sil.$_{wt\%}$ is total silicate (quartz and feldspar), and ρ is bulk density. The R^2-value for this model is 0.508 (Table 9), meaning that 50.8% of the variation in hardness can be explained by the independent

properties. If the model accounted for all the variation present, the R^2-value would be 1. While the standard error for both the constant and density is elevated compared to other variables (Table 8), this could be mitigated with more data and does not necessarily invalidate the equation.

Table 8: The results from multiple linear regression**.**

XRD vs Hardness					
	Coefficient	Std. error.	t	p	R^2
Constant	-141.01	174.28	-0.81	0.43	
Total Carbonate (wt.%)	2.05	0.94	2.17	0.04	0.06
Quartz + Feldspars (wt.%)	4.58	1.13	4.07	$3.9x10^{-4}$	0.24
Density (g/cm^3)	198.80	60.61	3.28	$3.0x10^{-3}$	0.11

Table 9: Statistics for above multivariate regression**.**

Statistics of Equation	
Dependent variable:	Average Median Hardness (HLD)
Number:	30
Model R^2:	0.51

MLR of UCS

An exponential relationship exists that relates hardness to UCS (Figure 22) and takes the general form:

$$UCS = n * e^{(f*HLD)}$$

where: *n* is the y-intercept, *f* is a constant, and HLD is hardness. RMSE, *n*, and *f* were examined for: average hardness, perpendicular hardness, and parallel hardness as they related to UCS. The distribution of *n* became non-normal after the eleventh iteration for average hardness (Appendix 3). Data distribution for perpendicular hardness remained normal through 20 iterations (Appendix 3). Similar to average hardness, *n* became non-

normal after 12 iterations (Appendix 3). Thus, mean values of *n* and *f* were used to develop equations predicting UCS from hardness (Figure 22).

The RMSE of each model were compared against each other to see which model best predicted UCS (Appendix 3). The equation using average hardness had the lowest RMSE at 36.88 MPa, whereas the equation using parallel hardness had the highest RMSE at 43.16 MPa (Appendix 3). The model using perpendicular hardness had a RMSE of 37.23 MPa, indicating that it was better at predicting UCS than parallel hardness, but not better than using average hardness (Appendix 3). Visually, the best correlation between the curves and data exists in mid-ranges (500-700 HLD) in each model, but larger errors occur at either extreme (Figure 22). Therefore, a general equation predicting UCS from hardness may not be completely suitable for a mixture of strong and weak rocks. However, the models do indicate that either perpendicular hardness or average hardness are better predictors of UCS than parallel hardness.

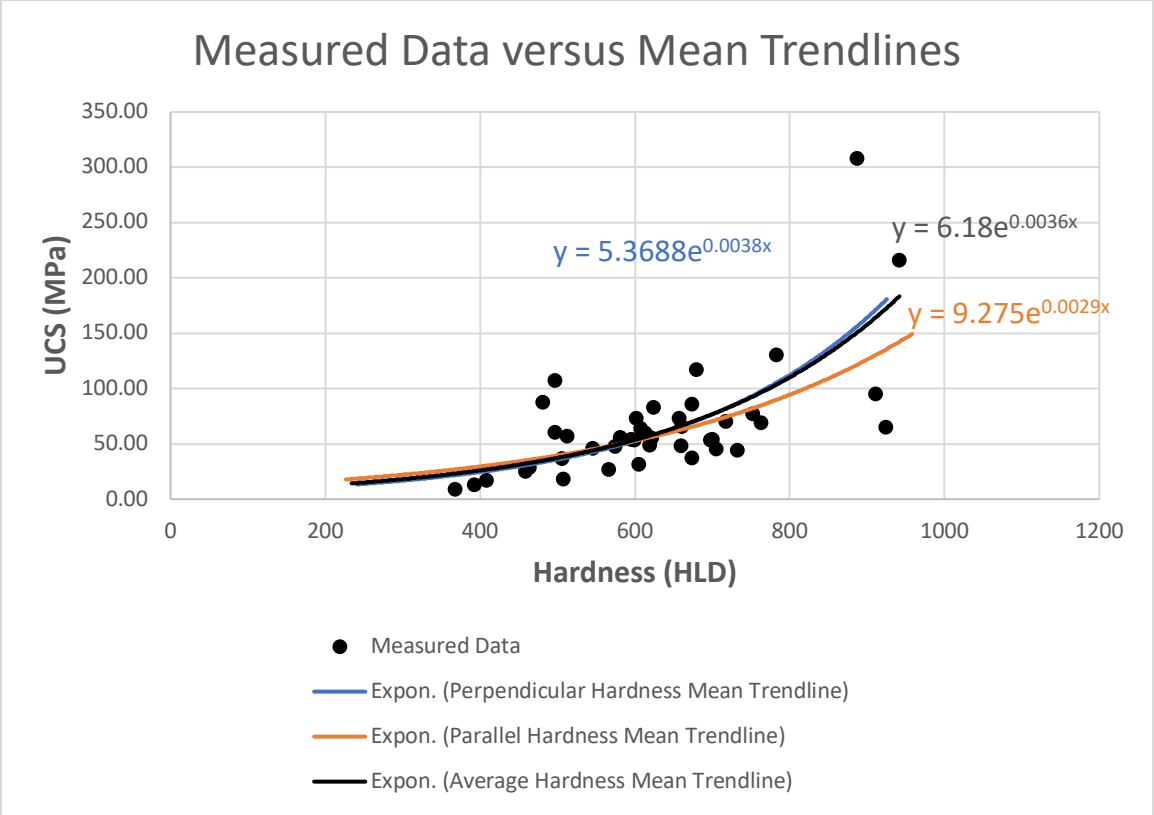

Figure 22: Model equations relating hardness to UCS with respect to the measurement direction.

Measured Results versus Predicted Results

After MLR was used to examine factors controlling hardness values, predicted values and measured values were compared (Figure 23). UCS predictions from prior research (Verwaal and Mulder, 1993; Meulenkamp, 1997; Aoki and Matsukura, 2008; Zahm and Enderlin, 2010; Lee et al., 2014) were also compared to this study's model.

Measured Hardness versus Predicted Hardness

Predicted hardness values were compared to measured values (Figure 23). Of the 30 samples used to develop the hardness equation, 20% have measured values close to predicted values: NMA2-1, NMA1-5, NMA1-15, OKST1-12, OKST1-4, and OKST1-14 (Figure 23). The range of the measured hardness for these six samples is 545.4-887.3

HLD, whereas the overall range of measured values is 295.5-941.8 HLD (Figure 23). Generally higher measured values are underpredicted and lower measured values are overpredicted (Figure 23).

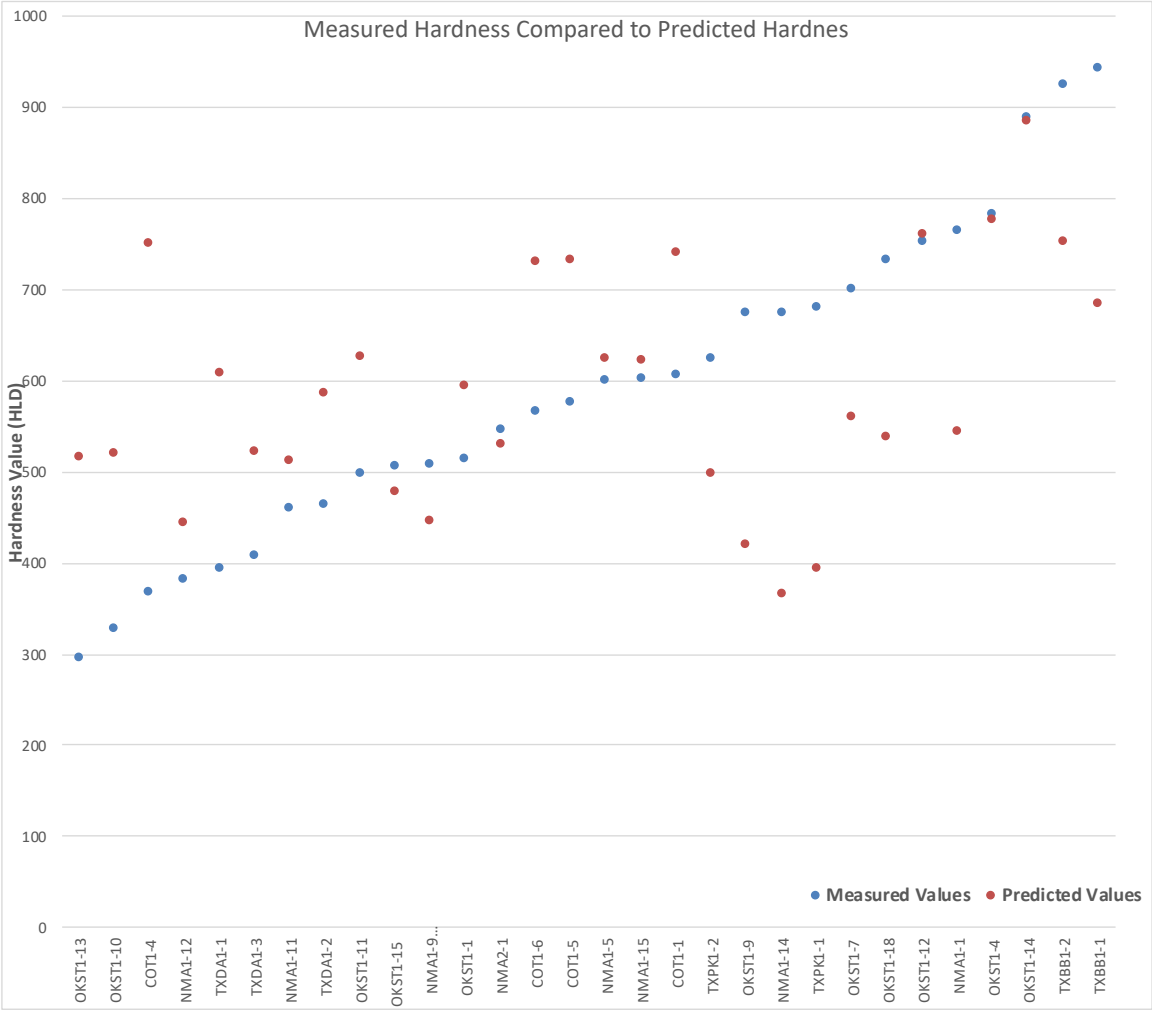

Figure 23: Measured hardness values compared to predicted hardness values**.**

Measured UCS versus Predicted UCS

Measured UCS values were compared with UCS predictions from this study and prior studies (Verwaal and Mulder, 1993; Meulenkamp, 1997; Aoki and Matsukura, 2008; Zahm and Enderlin, 2010; Lee et al., 2014) (Figure 24). The lowest R^2-values comes from Zahm and Enderlin (2010) because their model returned negative values for

soft rocks (Figure 24). UCS predictions from this study have the highest R^2-values (Figure 24) which is reasonable because the model is based on measured data from this study. No other UCS models have an R^2-value close to the one from this study, which is reinforced by each model's RMSE. The lowest RMSE comes from this study, whereas the highest RMSE comes from Verwaal and Mulder's (1993) model (Appendix 4).

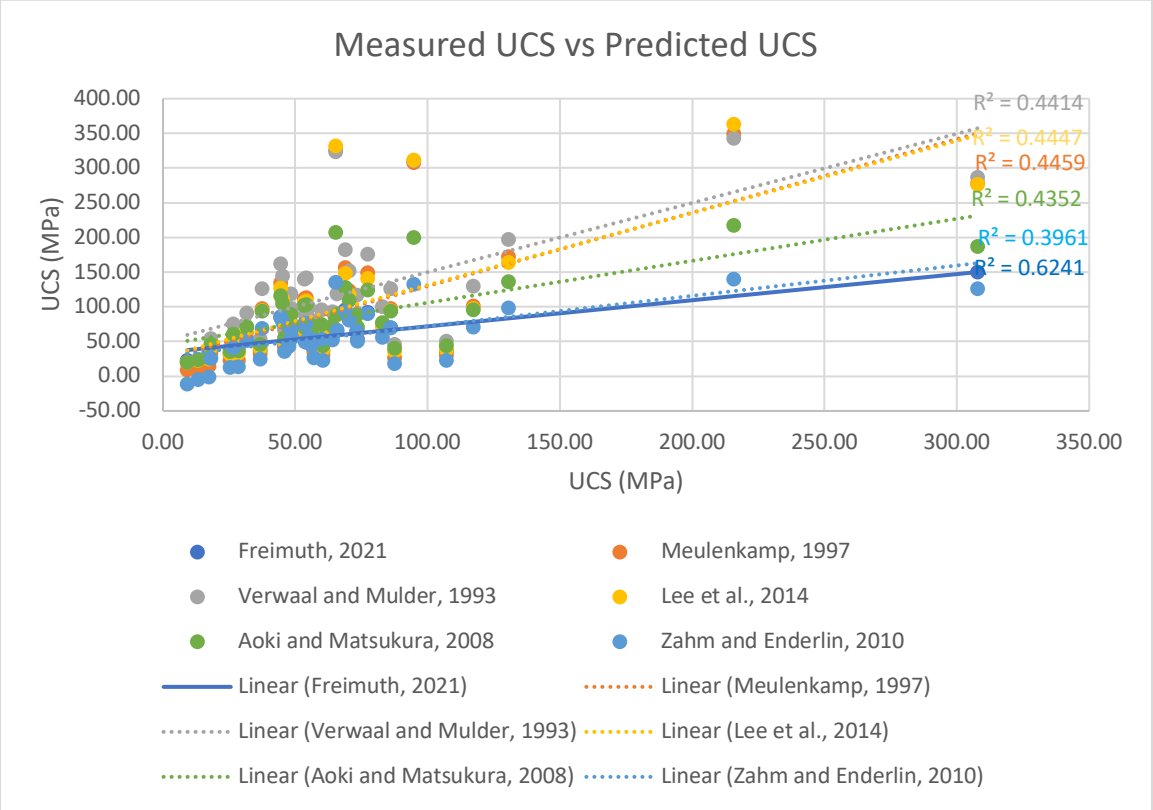

Figure 24: Results of UCS predictions compared to measured values**.**

Chapter 4: Discussion

Sample Holders

Few studies examine sample holders and their impacts on hardness measurements (e.g., Okawa et al., 1999; Corkum et al., 2018; Yilmaz and Goktan, 2018b). Yilmaz and Goktan (2018b) found that V-shaped core holders consistently returned lower hardness values than their U-shaped counterparts. However, these authors do not discuss the method of Bambino calibration. Often the tabletop is used for both calibration block and sample (e.g., Corkum et al., 2017). In such instances any error in readings could be systematic and thus a correction factor calculated because the block, which has a known hardness, and samples will be equally affected. For consistency, if sample holders can affect hardness readings, then the block should be mounted or secured in the same manner as the samples. Thus, questions arise about the data quality when mounting methods differ between samples and the calibration block, specifically whether the tool is measuring absolute hardness or relative hardness. For certain studies, relative hardness may suffice if a researcher is merely examining the relative change between materials, such as in a core study. However, if hardness will be linked to other absolute measurements (e.g., UCS), it is imperative to know a sample's true hardness rather than its relative hardness.

The main issue with assessing published research is that calibration protocols are typically not described. Data from this study show that both the tabletop and vise suffice as sample holders and for obtaining reproducible results. Furthermore, the data represent absolute hardness values since samples and the calibration block were secured in the same fashion.

Mechanical Hardness vs. Independent Properties

Previous research found that moisture content in a rock has an inverse relationship to hardness (Viles et al., 2011; Szilagyi et al., 2015; Desarnaud et al., 2019). Desarnaud et al. (2019) found that higher moisture contents led to decreases in hardness of up to 26%. Over 75% of samples analyzed in this study experienced hardness increases as a result of drying (Figure 12). On average, rocks in this project experienced a 4% increase in hardness due to drying, with hardness increasing more in rocks that lost water mass (Figure 11; Figure 12). Shales and silty shales experienced the largest increase in hardness due to drying, which potentially reflects the role of moisture content in rocks with well-defined laminations (Figure 12). Although the reasons for increasing hardness in this study cannot be linked solely to water loss, evidence exists suggesting water saturation affects hardness measurements (Figure 11; Figure 12). If possible, water content should be quantified when testing rock samples, especially when working on outcrop or when surface moisture is present. Furthermore, samples should be tested in their original state followed by renewed testing after drying in a lab setting.

In addition to the inverse relationship between water content and hardness, previous research also shows a negative correlation between hardness and porosity (e.g., Meulenkamp and Grima, 1999; Aoki and Matsukura, 2008; Brooks et al., 2016; Yilmaz and Goktan, 2018a). Porosity is also inversely correlated to hardness in this study (Table 6). It should be noted that various methods can be used to determine sample porosity (e.g., Aoki and Matsukura, 2008; Heidari et al., 2014; Aghamelu and Amah, 2017; Yilmaz and Goktan, 2018a). Water immersion porosimetry was used in this study,

resulting in the measurement of effective porosity. Effective porosity tends to be lower than true porosity because water is not forced into all available pores (Manger, 1963). These smaller values could be obscured by other factors controlling hardness during MLR analysis, causing effective porosity to be excluded as a factor despite a statistically significant relationship between porosity and hardness in SROC analysis (Table 6). Regardless, the inverse relationship between effective porosity and hardness suggests that water immersion porosimetry is a valid determination method. Also, correlations between effective porosity, hardness, and strength validate previous studies (e.g., Aoki and Matsukura, 2008; Heidari et al., 2014; Aghamela and Amah, 2017; Yilmaz and Goktan, 2018a). However, more work is needed to examine the variation between porosimetry methods and their control on hardness.

Anisotropy as it relates to mechanical hardness is mentioned in previous research (e.g., Verwaal and Mulder, 1993; Aydin, 2008; Murray, 2015), but never quantified. Rather, previous research notes that hardness reflects a rock's intrinsic anisotropy (e.g., Verwaal and Mulder, 1993; Aydin, 2008; Murray, 2015). Research concerning rock strength, however, found anisotropy to be dependent on the presence of elongate minerals such as clays and micas (Saroglou and Tsiambaos, 2007; Vakili et al., 2014). Saroglou and Tsiambaos (2007) suggest that rock strength can be fairly to highly anisotropic due to elongate minerals and defined bedding planes. In this study shales, conglomerates, and mudrocks were more anisotropic with respect to hardness than other groups and the aggregate anisotropy (Figure 14; Appendix 2). Specifically, conglomerates, mudrocks, and shales have median values that are anywhere from 4-7.5% higher than the aggregate median with other groups only differing by 1-2 % compared to the same aggregate

median (Appendix 2). However, strength anisotropy as determined by others (e.g., Saroglou and Tsiambaos, 2007; Vakili et al., 2018) must be inferred from the correlation between hardness and UCS (Figure 19). There is evidence that hardness anisotropy relates to strength anisotropy because perpendicular hardness correlated more strongly to UCS than parallel hardness (Figure 19). If this was not the case, then both perpendicular hardness and parallel hardness would have the same R^2-value compared to UCS. Thus, hardness anisotropy might be useful as a proxy for strength anisotropy, but further work is needed to fully validate this hypothesis.

Several studies have shown that density is positively correlated to mechanical hardness (e.g., Meulenkamp and Grima, 1999; Yilmaz, 2013; Yilmaz and Goktan, 2018a). Meulenkamp and Grima (1999) found that higher densities correspond to higher hardness values and ultimately higher UCS values. Similarly, Yilmaz and Goktan (2018a) show a positive correlation between hardness and density. Yilmaz (2013) explicitly states that the inclusion of density data leads to better predictions of UCS from hardness data. Based on data from this study, a statistically significant positive relation exists between hardness and density. Furthermore, density can be used to predict sample hardness (Table 8). Thus, density data are critical in future studies because density partially controls mechanical hardness.

Several previous studies focused on the role of volume relative to mechanical hardness (e.g., Yilmaz, 2013; Lee et al., 2014; Brooks et al., 2016; Colwell, 2017; Corkum et al., 2018; Lee, 2018). For example, Brooks et al. (2016) proposed 197 cm^3 as the minimum volume necessary to obtain valid hardness data, whereas Corkum et al. (2018) proposed a minimum volume of no less than 90 cm^3. While the recommended

minimum volume varies, there is an agreement that hardness values will increase with volume up to a certain point after which hardness does not vary significantly (Brooks et al., 2016; Corkum et al., 2018). Despite these observations, the relationship between sample volume and hardness is not statistically significant in my data (Table 6), possibly due to the large size of samples used in the study (Figure 16). The goal of this study was to examine intrinsic properties and their relation to mechanical properties. Thus, the lack of correlation between sample volume and hardness indicates sample volumes were large enough to preclude variations in hardness.

Relations between hardness and mineralogy are mentioned explicitly or implicitly by several previous studies (e.g., Meulenkamp and Grima, 1999; Kawasaki, 2002; Zahm and Enderlin, 2010; Brooks et al., 2016; Dong et al., 2017; Zhou et al., 2018; Celik and Cobanoglu, 2019). Some workers explicitly tie mineralogy to rock hardness stating that certain minerals such as calcite are harder than others, such as clays (e.g., Zahm and Enderlin, 2010; Celik and Cobanoglu, 2019). Yet others discuss the relationship between hardness and mineralogy implicitly (e.g., Brooks et al., 2016) by comparing the lithology of a sample to its corresponding hardness and then drawing conclusions from groups of similar lithologies. The present study analyzed sample mineralogy and compared it to hardness, thereby explicitly linking mineralogy to hardness. MLR shows that both silicate content and carbonate content control hardness (Table 8), whereas SROC shows that only quartz+feldspar content is related to hardness (Table 7). Despite this discrepancy, there is a qualitative, hierarchical relationship between mineralogy and mechanical properties (Figure 20). While silica content appears to be linked with the hardest and strongest rocks, there are silica-rich rocks that are soft and weak (Figure 13; Figure 18). Thus, the

relationship between mineralogy and mechanical properties is not definitive. However, this probably means that mineralogy is further influenced by other properties and it is not the sole controlling factor for mechanical hardness. Mineralogical analyses should continue in future research to fully quantify the relationship between mineralogy and hardness, because this relationship is not yet well enough understood beyond a qualitative level.

Ultimately, many studies have established the relation between hardness and UCS (e.g., Verwaal and Mulder, 1993; Aoki and Matsukura, 2008; Celik and Cobanoglu, 2019; Desarnaud et al., 2019) as hardness measurements provide a quick and inexpensive way to determine material strength. Previous research shows that hardness correlates positively with UCS (e.g., Verwaal and Mulder, 1993; Aoki and Matsukura, 2008; Celik and Cobanoglu, 2019; Desarnaud et al., 2019), which is also supported by this study (Figure 19; Figure 22). Like previous studies (Verwaal and Mulder, 1993; Meulenkamp, 1997; Aoki and Matsukura, 2008; Zahm and Enderlin, 2010; Lee et al., 2014) an empirical equation predicting UCS from hardness values was derived. Comparisons of the results (Figure 24) shows that the applicability of these equations are specific to their data. Based on this, one can draw the following conclusions: 1) this study's model sufficiently predicts UCS from hardness, and 2) previous equations may not be applicable to other datasets. To improve the fit of the equation, additional variables may need to be incorporated. Adding properties such as density and porosity can account for variations in the data that hardness alone cannot (e.g., Yilmaz, 2013). Thus, while the correlation between hardness and strength can be sufficient, in order to fully characterize a rock,

other properties must be measured and incorporated into models when predicting strength from hardness.

UCS vs. Independent Properties

Previous research by Grima and Babuska (1999) and others (e.g., Yilmaz, 2013; Yilmaz and Goktan, 2018a) found a positive correlation between density and UCS. Yilmaz (2013) used density to improve the fit between hardness and strength, as did Grima and Babuska (1999) and Meulenkamp and Grima (1999). The present study shows that density and UCS are positively correlated in a statistically significant manner (Table 6). Thus, positive correlation between density and UCS continues to be shown and density remains one of the most important variables with respect to UCS because density is an aggregate of sample's bulk mineralogy and porosity. Therefore, a change in either mineralogy or porosity through a process like dissolution will be reflected in the density of a sample, and ultimately the UCS.

The presence of clay and its correlation to low UCS has previously been documented (e.g., Rutter et al., 2017; Heap et al., 2018; Vazquez et al., 2018). Generally, new data presented here show that UCS decreases with increasing amounts of clay. Two samples with high clay content (NMA1-12; OKST1-13) proved impossible to core for UCS testing. While these results do not quantitatively prove a relationship between mineralogy and UCS, higher UCS values are documented in silica-rich rocks and carbonate-rich rocks compared to clay-rich rocks (Figure 20). Thus, results from the present study support previous findings.

Statistical Analyses

Existing studies attempted to determine the best manner to statistically treat hardness data from the Bambino (e.g., Tiryaki, 2008; Viles et al., 2011; Wilhelm et al., 2016; Yilmaz and Goktan, 2018b). Many researchers opted to trim outliers from their data (e.g., Zahm and Enderlin, 2010; McClave, 2014; Murray, 2015). As Yilmaz (2013) and Wilhelm et al. (2016) discuss, trimming outliers potentially leads to datasets that do not fully characterize a sample. McClave (2014) excluded any readings that deviated by more than 10% from the previous reading. Rather than trim outliers, this study used median values as suggested by Wilhelm et al. (2016). Utilizing SROC (Table 6; Table 7) led to results that validated Wilhelm et al.'s (2016) research.

In addition, the calibration block for hardness measurement can yield non-normal data, necessitating the use of median values during calibration (Table 3). This brings into question the ASTM-A956 (2006) standard, which recommends the arithmetic mean of two measurements during calibration checks. Although the calibration block should not yield values that deviate too far from the engraved value, measured values at times deviated by more than 6 HLD units even though the Bambino used in this study was recently checked and recalibrated. Thus, researchers might conclude a Bambino is out of calibration based on two anomalous readings, when the data is non-normal and median values should be used instead. To follow ASTM recommendations, an arithmetic mean should still be calculated during calibration because it is a value often reported in the literature (e.g., Zahm and Enderlin, 2010; McClave, 2014; Murray, 2015). Based on the results of this study median values are recommended in future studies.

MLR has been used with varying degrees of success (e.g., Grima and Babuska, 1999; Kilic and Teyman, 2008; Armaghani et al., 2016. Based on statistical analyses presented here, MLR is useful for identifying independent variables controlling hardness (Figure 24). Results here are in agreement with previous research (Figure 24). While MLR is an extremely useful analytical tool, care must be taken during data collection and processing to yield accurate results. For example, Armaghani et al. (2016) produced low R^2-values in their research possibly due to: operator variance, heterogeneity of the samples, or other factors. Thus, the potential for error should be mitigated when taking measurements so that the results of MLR are valid.

Although PCA were conducted, results are not overly informative (Figure 21). The data groupings did not reveal any previously obscured groupings (Figure 21). While Tiryaki (2008) used PCA with good results, PCA results compiled in the present study were not as encouraging.

Chapter 6: Conclusions

This study examined the correlation between mechanical hardness, strength, and their controlling factors. Several independent properties were measured (density, effective porosity, volume, bulk mineralogy, and water saturation) and statistically compared against corresponding mechanical properties.

The first question examined was the preferred method to secure samples during hardness testing. Through statistical analyses, both the large metal vise and table top proved sufficient for securing samples because both returned accurate values of the steel calibration block.

The second question addresses the independent rock properties that control mechanical hardness. This study shows that density, effective porosity, water content, and mineralogy all exert control on mechanical hardness. Also, mechanical hardness is closely related to mechanical strength validating previous studies.

Third, hardness anisotropy is shown to relate to lithology. Also, the direction of hardness measurements is shown to correlate differently to UCS. Thus, hardness anisotropy could serve as a useful proxy for strength anisotropy, but further work is needed to quantify this relationship.

Finally, XRD analysis should be included in future geomechanical studies because mineralogy exerts control on mechanical properties. Evidence exists that silicates and carbonates are positively correlated to mechanical properties, whereas clay content is negatively correlated. However, it appears that hardness does not depend solely on mineralogical properties as effective porosity and density might also play a role.

Chapter 7: References

Aghamelu, O. P., & Amah, J. I. (2017). Quality and durability of some marble deposits in the southern schist belt (Nigeria) as construction stones. Bulletin of Engineering Geology and the Environment, 76(4), 1563-1575.

Alberti, A. P., Gomes, A., Trenhaile, A., Oliveira, M., & Horacio, J. (2013). Correlating river terrace remnants using an Equotip hardness tester: An example from the Miño River, northwestern Iberian Peninsula. Geomorphology, 192, 59-70.

Aoki, H., & Matsukura, Y. (2008). Estimating the unconfined compressive strength of intact rocks from Equotip hardness. Bulletin of Engineering Geology and the Environment, 67(1), 23-29.

Armaghani, D. J., Mohamad, E. T., Hajihassani, M., Yagiz, S., & Motaghedi, H. (2016). Application of Several Non-linear Prediction Tools for Estimating Uniaxial Compressive Strength of Granitic Rocks and Comparison of their Performances. Engineering with Computers, 32, 189–206.

Asiri, Y. (2017). Standardized Process for Field Estimation of Unconfined Compressive Strength Using Leeb Hardness. (Master of Applied Science), Dalhousie University, Halifax, Nova Scotia.

ASTM. (2006). Standard Test Method for Leeb Hardness Testing of Steel Products. ASTM A956-06. ASTM Book of Standards, West Conshoshocken, PA.

ASTM. (2010). Standard test method for compressive strength and elastic moduli of intact rock core specimens under varying states of stress and temperature. ASTM D7012-10. ASTM Book of Standards, West Conshoshocken, PA.

Aydin, A. (2008). ISRM suggested method for determination of the Schmidt hammer rebound hardness: revised version. In The ISRM Suggested Methods for Rock Characterization, Testing and Monitoring: 2007-2014 (pp. 25-33): Springer.

Broitman, E. (2017). Indentation hardness measurements at macro-, micro-, and nanoscale: A critical overview. Tribology Letters, 65(1), 1-18.

Brooks, D., Janson, X., & Zahm, C. (2016). The effect of sample volume on micro-rebound hammer UCS measurements in Gulf Coast Cretaceous carbonate cores. Gulf Coast Association of Geological Societies Journal, 5, 189-202.

Çelik, S. B., & Çobanoğlu, İ. (2019). Comparative investigation of Shore, Schmidt, and Leeb hardness tests in the characterization of rock materials. Environmental Earth Sciences, 78(18), 553-569.

Colwell, C. L. (2018). Correlation of chemostratigraphy, mechanical stratigraphy, and total organic carbon using one core from the Barnett Shale, Fort Worth Basin, Hood County, Texas. (Master of Science), Texas Christian University, Fort Worth, Texas.

Coombes, M. A., Feal-Pérez, A., Naylor, L. A., & Wilhelm, K. (2013). A non-destructive tool for detecting changes in the hardness of engineering materials: Application of the Equotip durometer in the coastal zone. Engineering Geology, 167, 14-19.

Corkum, A., Asiri, Y., Naggar, H., & Kinakin, D. (2018). The Leeb Hardness Test for Rock: An Updated Methodology and UCS Correlation. Rock mechanics and rock engineering, 51, 665-675.

Daniels, G., McPhee, C. A., Sorrentino, Y. C., & McCurdy, P. (2012). Non-destructive strength index testing applications for sand failure evaluation. Paper presented at the SPE Asia Pacific Oil and Gas Conference and Exhibition.

Demirdag, S., Yavuz, H., & Altindag, R. (2009). The effect of sample size on Schmidt rebound hardness value of rocks. International Journal of rock mechanics and mining sciences, 46(4), 725-730.

Desarnaud, J., Kiriyama, K., Bicer Simsir, B., Wilhelm, K., & Viles, H. (2019). A laboratory study of Equotip surface hardness measurements on a range of sandstones: What influences the values and what do they mean? Earth Surface Processes and Landforms, 44(7), 1419-1429.

Dong, T., Harris, N. B., Ayranci, K., & Yang, S. (2017). The impact of rock composition on geomechanical properties of a shale formation: Middle and Upper Devonian Horn River Group shale, Northeast British Columbia, Canada. AAPG Bulletin, 101(2), 177-204.

Golodkovskaia, G. A., Krasilova, N. S., Ladygin, V. M., & Shaumian, L. V. (1975). Factors controlling solid rock strength. Bulletin of Engineering Geology and the Environment, 11(1), 65-69.

Grima, M. A., & Babuška, R. (1999). Fuzzy model for the prediction of unconfined compressive strength of rock samples. International Journal of Rock Mechanics and Mining Sciences, 36(3), 339-349.

Hack, H., Hingira, J., & Verwaal, W. (1993). Determination of discontinuity wall strength by Equotip and ball rebound tests. Paper presented at the International Journal of Rock Mechanics and Mining Sciences and Geomechanics Abstracts, 30(2), 151-155.

Hack, R., & Huisman, M. (2002). Estimating the intact rock strength of a rock mass by simple means. Paper presented at the Proceedings 9th Congress of the International Association for Engineering Geology and the Environment, Durban, South Africa.

Hansen, C. D., Meiklejohn, K. I., Nel, W., Loubser, M. J., & Van Der Merwe, B. J. (2013). Aspect-controlled weathering observed on a blockfield in Dronning Maud Land, Antarctica. Geografiska Annaler: Series A, Physical Geography, 95(4), 305-313.

Hauff, P. L., Starkey, H. C., Blackmon, P. D., & Pevear, D. R. (1984). Sample preparation procedures for the analysis of clay minerals by X-ray diffraction. United States Geological Survey Open File Report 82-934, 1-62.

Heap, M.J., Farquharson, J.I., Kushnir, A.R.L., Lavallee, Y., Baud, P., Gilg, H.A., & Reuschle, T. (2018). The influence of water on the strength of Neapolitan Yellow Tuff, the most widely used building stone in Naples (Italy). Bulletin of Volcanology, 80(51), 51-66.

Hammer, Ø., Harper, D.A.T., & Ryan, P.D. (2001). PAST: Paleontological statistics software package for education and data analysis. Palaeontologia Electronica 4(1): 9pp. http://palaeo-electronica.org/2001_1/past/issue1_01.htm

Heidari, M., Khanlari, G.R., Torabi-Kaveh, M., Kargarian, S., Sanaie, S. (2014). Effect of Porosity on Rock Brittleness. Rock Mechanics and Rock Engineering, 47, 785–790.

Hoek, E. (1977). Rock mechanics laboratory testing in the context of a consulting engineering organization. Paper presented at the International Journal of Rock Mechanics and Mining Sciences & Geomechanics Abstracts, 14(2), 93-101.

Hoek, E. & Brown, E.T. (1980). Underground excavations in rock. Institution of Mining and Metallurgy. London: Chapman & Hall.

Hudson, J. A., & Harrison, J. P. (1997). Engineering Rock Mechanics: An Introduction to the Principles. ProQuest Ebook Central https://ebookcentral.proquest.com

Kahraman, S. (2001). Evaluation of simple methods for assessing the uniaxial compressive strength of rock. International Journal of Rock Mechanics and Mining Sciences, 38(7), 981-994.

Kawasaki, S., Tanimoto, C., Koizumi, K., & Ishikawa, M. (2002). An Attempt to Estimate Mechanical Properties of Rocks Using the Equotip Hardness Tester. Journal of the Japan Society of Engineering Geology, 43, 244-248.

Kiliç, A., & Teymen, A. (2008). Determination of Mechanical Properties of Rocks Using Simple Methods. Bulletin of Engineering Geology and the Environment, 67, 237-244.

Lee, J., Smallwood, L., & Morgan, E. (2014). New application of rebound hardness numbers to generate logging of unconfined compressive strength in laminated shale formations. Paper presented at the 48th US rock mechanics/geomechanics symposium.

Leeb, D. (1979). Dynamic hardness testing of metallic materials. NDT International, 12(6), 274-278.

Manger, G. E. (1963). Porosity and bulk density of sedimentary rocks. Bulletin Number 1144-E. Washington, D.C: United States Department of the Interior, Geological Survey.

Manouchehrian, A., Sharifzadeh, M., Moghadam, R.H., Nouri, T. (2012). Selection of regression models for predicting strength and deformability properties of rocks using GA. International Journal of Mining Science and Technology. 23(4), 495-501.

McClave, G. A. (2014). Correlation of rebound-hammer rock strength with core and sonic-log derived mechanical rock properties in Cretaceous Niobrara and frontier formation cores, Piceance Basin, Colorado. Paper presented at the Unconventional Resources Technology Conference, Denver, Colorado, 25-27 August 2014.

Meulenkamp F. (1997). Improving the prediction of the UCS, by Equotip readings using statistical and neural network models. Memoirs of the Centre for Engineering Geology in the Netherlands.162-127.

Meulenkamp, F., & Grima, M. A. (1999). Application of neural networks for the prediction of the unconfined compressive strength (UCS) from Equotip hardness. International Journal of Rock Mechanics and Mining Sciences, 36(1), 29-39.

Murray, C. D. (2015). Mechanical stratigraphy and sonic log relationships using the Proceq Bambino in the Niobrara Formation, Denver Basin. (Master of Science), Colorado School of Mines, Golden, Colorado.

Okan, S., & Momayez, M. (2017). Correlation Between Equotip Hardness Index, Mechanical Properties and Drillability of Rocks. Dokuz Eylül Üniversitesi Mühendislik Fakültesi Fen ve Mühendislik Dergisi, 19(56), 519-531.

Okawa, S., Ohoka, M., Funato, A., (1999). Application of hardness tester to rock specimens. Proceedings of the 29th symposium of rock mechanics. 256–260.

Rezaei, M., Majdi, A., & Monjezi, M. (2014). An intelligent approach to predict unconfined compressive strength of rock surrounding access tunnels in longwall coal mining. Neural Computing and Applications, 24(1), 233-241.

Ritz, E., Honarpour, M. M., Dvorkin, J., & Dula, W. F. (2014). Core Hardness Testing and Data Integration for Unconventionals. Paper presented at the SPE/AAPG/SEG Unconventional Resources Technology Conference.

Rutter, E., Mecklenburgh, J., & Taylor, K. (2017). Geomechanical and Petrophysical Properties of Mudrocks: Introduction. Geological Society, London, Special Publications, 454(1), 1-13.

Saroglou, H., & Tsiambaos, G. (2007). Classification of anisotropic rocks. Paper presented at 11th Congress of the International Society for Rock Mechanics, International Society for Rock Mechanics and Rock Engineering, Lisbon, Portugal, 1, 1-6.

Shalabi, F. I., Cording, E. J., & Al-Hattamleh, O. H. (2007). Estimation of rock engineering properties using hardness tests. Engineering Geology, 90(3-4), 138-147.

Szilágyi, K., Borosnyói, A., & Zsigovics, I. (2015). Understanding the rebound surface hardness of concrete. Journal of Civil Engineering and Management, 21(2), 185-192.

Taylor, C. Z. (2017). Chemostratigraphy, Mechanical Stratigraphy, and Sample Size Influence on Micro-Mechanical Tests for Two Barnett Shale Cores, Fort Worth Basin, Texas.

Tiryaki, B. (2008). Predicting intact rock strength for mechanical excavation using multivariate statistics, artificial neural networks, and regression trees. Engineering Geology, 99(1), 51-60.

Tuncay, E., & Hasancebi, N. (2009). The effect of length to diameter ratio of test specimens on the uniaxial compressive strength of rock. Bulletin of Engineering Geology and the Environment, 68(4), 491-497.

Tuncay, E., Ozcan, N. T., & Kalender, A. (2019). An approach to predict the length-to-diameter ratio of a rock core specimen for uniaxial compression tests. Bulletin of Engineering Geology and the Environment, 78(7), 5467-5482.

Vakili, A., Albrecht, J., Sandy, M. (2014). Rock Strength Anisotropy and Its Importance in Underground Geotechnical Design. Third Australasian Ground Control in Mining Conference. 1-14.

Vazquez, P., Sánchez-Delgado, N., Carrizo, L., Thomachot-Schneider, C., Alonso, F.J. (2018). Statistical approach of the influence of petrography in mechanical properties and durability of granitic stones. Environmental Earth Sciences, 77 (7), 1-17.

Verwaal, W., & Mulder, A. (1993). Estimating rock strength with the Equotip hardness tester. International Journal of Rock Mechanics and Mining Sciences and Geomechanics Abstracts, 30(6), 659-662.

Viles, H., Goudie, A., Grab, S., & Lalley, J. (2011). The use of the Schmidt Hammer and Equotip for rock hardness assessment in geomorphology and heritage science: a comparative analysis. Earth Surface Processes and Landforms, 36(3), 320-333.

Wilhelm, K., Viles, H., & Burke, Ó. (2016). Low impact surface hardness testing (Equotip) on porous surfaces–advances in methodology with implications for rock weathering and stone deterioration research. Earth Surface Processes and Landforms, 41(8), 1027-1038.

Yaşar, E., & Erdoğan, Y. (2004). Estimation of rock physicomechanical properties using hardness methods. Engineering Geology, 71(3-4), 281-288.

Yılmaz, N. G. (2013). The influence of testing procedures on uniaxial compressive strength prediction of carbonate rocks from Equotip hardness tester (EHT) and proposal of a new testing methodology: Hybrid dynamic hardness (HDH). Rock mechanics and rock engineering, 46(1), 95-106.

Yilmaz, N. G., & Goktan, R. (2018a). Comparison and combination of two NDT methods with implications for compressive strength evaluation of selected masonry and building stones. Bulletin of Engineering Geology and the Environment, 78(6), 4493-4503.

Yilmaz, N. G., & Göktan, R. M. (2018b). Analysis of the Leeb hardness test data obtained by using two different rock core holders. Süleyman Demirel Üniversitesi Fen Bilimleri Enstitüsü Dergisi, 22(1), 24-31.

Yüksek, S. (2019). Mechanical properties of some building stones from volcanic deposits of mount Erciyes (Turkey). Materiales de Construcción, 69(334), 187.

Zahm, C. K., & Enderlin, M. (2010). Characterization of rock strength in Cretaceous strata along the Stuart City Trend, Texas: Gulf Coast Association of Geological Societies Transactions, 60, 693–702.

Zhou, J., Mandal, S., Chen, F., Quest, & Hume, D. (2018). Reservoir Geomechanic Heterogeneity Index (RGHI): Concept, Methodology, and Application. Paper presented at the Unconventional Resources Technology Conference, Houston, Texas, 23-25 July 2018.

Appendix 1

Box Name	Box 1 (HLD 768)	Box 1 (HLD 769)	Box 1 (HLD 768)	Box 1 (HLD 769)
Given Hardness	**768**	**769**	**768**	**769**
Holding Apparatus	**Vise**	**Vise**	**Table**	**Table**
Test No.				
1	779	791	791	773
2	774	768	778	763
3	777	848	779	765
4	767	770	774	763
5	775	771	777	768
6	780	771	817	766
7	771	770	781	767
8	775	767	774	766
9	773	770	776	771
10	775	770	840	768
11	771	771	776	770
12	770	767	774	763
13	764	768	774	770
14	770	762	776	767
15	767	767	770	771
16	772	770	772	770
17	771	759	779	765
18	778	768	771	766
19	765	770	774	771
20	777	767	781	770
21	764	773	777	769
22	770	771	769	764
23	769	766	777	770
24	769	767	769	765
25	746	771	775	770
26	769	773	769	771
27	777	775	772	768
28	767	770	774	771
29	764	774	778	770
30	780	774	773	771
31	770	763	780	771

Box Name	Box 1 (HLD 768)	Box 1 (HLD 769)	Box 1 (HLD 768)	Box 1 (HLD 769)
Given Hardness	**768**	**769**	**768**	**769**
Holding Apparatus	**Vise**	**Vise**	**Table**	**Table**
32	775	771	776	771
33	772	771	771	778
34	773	768	772	771
35	770	771	778	771
36	770	766	786	771
37	774	771	773	767
38	774	768	770	769
39	776	769	782	767
40	770	768	863	765
41	807	768	770	761
42	763	772	779	769
43	773	766	770	768
44	771	766	773	767
45	773	773	774	767
46	766	771	774	766
47	777	771	791	772
48	769	771	768	769
49	775	763	768	766
50	767	770	770	763
51	761	769	760	771
52	763	769	779	770
53	770	767	777	768
54	773	766	771	768
55	772	778	771	770
56	768	767	771	773
57	765	767	774	762
58	771	767	771	765
59	770	760	801	771
60	770	764	769	767
61	778	774	771	772
62	775	765	769	773
63	772	768	813	772
64	774	772	772	766
65	774	771	820	771
66	771	769	771	763

Box Name	Box 1 (HLD 768)	Box 1 (HLD 769)	Box 1 (HLD 768)	Box 1 (HLD 769)
Given Hardness	**768**	**769**	**768**	**769**
Holding Apparatus	**Vise**	**Vise**	**Table**	**Table**
67	760	841	775	769
68	765	765	776	772
69	761	891	768	768
70	769	768	772	769
71	770	772	777	771
72	774	769	776	769
73	771	766	773	769
74	762	772	793	766
75	778	771	739	770
76	766	773	778	769
77	771	772	768	769
78	774	770	774	770
79	767	771	772	764
80	770	771	773	767
81	779	769	770	767
82	767	770	771	771
83	779	771	782	771
84	815	771	768	765
85	764	771	773	768
86	768	765	777	769
87	759	766	780	772
88	770	764	771	771
89	778	766	769	770
90	776	769	771	767
91	771	767	771	767
92	812	772	774	772
93	772	766	771	770
94	771	772	777	770
95	773	768	769	770
96	841	765	771	769
97	762	770	791	766
98	774	770	772	773
99	769	770	772	767
100	771	770	776	767

Box 1				
	Vise 768	**Vise 769**	**Table 768**	**Table 769**
Number	100	100	100	100
Min	746	759	739	761
Max	841	891	863	778
Sum	77247	77193	77705	76857
Mean	772.47	771.93	777.05	768.57
Std. error	1.12	1.65	1.47	0.29
Variance	125.48	271.62	217.42	8.47
Stand. dev	11.20	16.48	14.75	2.91
Median	771	770	774	769
25 prcntil	768	767	771	767
75 prcntil	774.75	771	777.75	771
Skewness	3.44	5.65	3.30	-0.21
Kurtosis	17.27	34.36	15.23	0.38
Geom. mean	772.39	771.77	776.92	768.56
Coeff. var	1.45	2.14	1.90	0.38
Normality Tests				
	Vise 768	**Vise 769**	**Table 768**	**Table 769**
Number	100	100	100	100
Shapiro-Wilk W	0.65	0.34	0.61	0.96
p(normal)	4.32×10^{-14}	3.70×10^{-19}	6.26×10^{-15}	7.5×10^{-3}
Box 1 Wilcoxon Tests				
	Vise 768	**Vise 769**	**Table 768**	**Table 769**
Given median:	768	769	768	769
Sample median:	771	770	774	769
W :	3849.5	2418	4412.5	2283
Normal appr. z :	5.05	0.90	7.92	1.36
p (same median):	4.35×10^{-7}	0.37	2.32×10^{-15}	0.17
	Medians are significantly different	Medians are not significantly different	Medians are significantly different	Medians are not significantly different

Appendix 2

	Chalk	Conglomerate	Limestone	Mudrock	Novaculite	Shale	Sandstone	Silty Shale
Number	5	3	15	2	3	7	6	7
Min	0.84	1.04	0.87	0.97	0.97	0.68	0.97	0.85
Max	1.04	1.09	1.37	1.18	0.98	1.45	1.13	1.27
Sum	4.87	3.17	15.32	2.15	2.93	7.27	6.15	7.14
Mean	0.97	1.06	1.02	1.08	0.98	1.04	1.03	1.02
Std. error	0.04	0.02	0.03	0.11	0.00	0.10	0.02	0.05
Variance	0.01	0.00	0.02	0.02	0.00	0.07	0.00	0.02
Stand. dev	0.08	0.03	0.13	0.15	0.01	0.26	0.06	0.13
Median	0.99	1.04	0.99	1.08	0.98	0.97	1.01	1.02
25 prcntil	0.90	1.04	0.96	0.97	0.97	0.86	0.98	0.90
75 prcntil	1.04	1.09	1.03	1.18	0.98	1.31	1.07	1.06
Skewness	-1.37	1.73	1.77	0.00	-1.73	0.46	1.32	0.87
Kurtosis	1.80	-2.33	3.59	-2.75	-2.33	-0.49	1.63	1.71
Geom. mean	0.97	1.06	1.01	1.07	0.98	1.01	1.02	1.01
Coeff. var	8.45	2.73	12.35	13.81	0.59	25.50	5.75	13.17

Appendix 3

Average Hardness Summary Statistics			
	RMSE	n	f
Number	11	11	11
Shapiro-Wilk W	0.89	0.91	0.95
p(normal)	0.14	0.25	0.59
	RMSE	n	f
N	11	11	11
Min	23.11	3.21	2.70×10^{-3}
Max	50.03	10.33	4.50×10^{-3}
Sum	405.71	67.99	3.96×10^{-2}
Mean	36.88	6.18	3.60×10^{-3}
Std. error	3.20	0.73	1.87×10^{-4}
Variance	112.75	5.89	3.84×10^{-7}
Stand. dev	10.62	2.43	6.20×10^{-4}
Median	34.97	5.75	3.70×10^{-3}
25 prcntil	25.47	3.96	2.90×10^{-3}
75 prcntil	49.12	8.51	4.20×10^{-3}
Skewness	-0.05	0.66	-1.48×10^{-1}
Kurtosis	-1.72	-0.81	-1.25
Geom. mean	35.43	5.77	3.55×10^{-3}
Coeff. var	28.79	39.25	1.72×10^{1}

Perpendicular Hardness Summary Statistics			
Summary Statistics			
	RMSE	n	f
Number	20	20	20
Shapiro-Wilk W	0.91	0.94	0.96
p(normal)	0.07	0.21	0.60
	RMSE	n	f
N	20	20	20
Min	18.26	2.39	2.00×10^{-3}
Max	55.34	8.69	5.00×10^{-3}
Sum	744.68	107.38	7.54×10^{-2}
Mean	37.23	5.37	3.77×10^{-3}
Std. error	2.67	0.45	1.70×10^{-4}
Variance	142.26	4.07	5.75×10^{-7}
Stand. dev	11.93	2.02	7.58×10^{-4}
Median	37.70	5.32	3.70×10^{-3}
25 prcntil	25.14	3.24	3.18×10^{-3}
75 prcntil	49.43	6.71	4.45×10^{-3}
Skewness	-0.09	0.22	-2.87×10^{-1}
Kurtosis	-1.57	-1.06	6.63×10^{-2}
Geom. mean	35.28	4.99	3.69×10^{-3}
Coeff. var	32.03	37.59	20.11

Parallel Hardness Summary Statistics			
Summary Statistics			
	RMSE	n	f
Number	12	12	12
Shapiro-Wilk W	0.93	0.86	0.94
p(normal)	0.38	0.05	0.50
	RMSE	n	f
N	12	12	12
Min	23.85	5.32	1.80×10^{-3}
Max	73.68	19.10	3.70×10^{-3}
Sum	517.96	111.30	3.53×10^{-2}
Mean	43.16	9.28	2.94×10^{-3}
Std. error	4.55	1.22	1.75×10^{-4}
Variance	248.87	17.73	3.66×10^{-7}
Stand. dev	15.78	4.21	6.05×10^{-4}
Median	43.79	7.87	3.05×10^{-3}
25 prcntil	26.85	5.74	2.35×10^{-3}
75 prcntil	54.40	12.54	3.48×10^{-3}
Skewness	0.36	1.27	-5.23×10^{-1}
Kurtosis	-0.62	1.28	-8.00×10^{-1}
Geom. mean	40.48	8.54	2.88×10^{-3}
Coeff. var	36.55	45.39	20.57

Appendix 4

Sample Name	Median Hardness	Measured UCS	Freimuth 2021	Meulenkamp 1997	Verwaal and Mulder 1993	Lee et al., 2014	Aoki and Matsukura, 2008	Zahm and Enderlin, 2010
COT1-1	604.8	31.55	54.51	65.02	91.86	67.41	71.95	51.71
COT1-2	594.8	54.34	52.58	61.03	87.42	64.12	69.01	49.07
COT1-4	367.6	9.22	23.21	9.81	20.90	20.60	20.73	-10.93
COT1-5	574.4	47.56	48.87	53.45	78.81	57.91	63.25	43.69
COT1-6	566.0	26.68	47.41	50.55	75.44	55.53	60.97	41.47
NMA1-1	762.8	68.94	96.28	157.07	183.20	148.52	128.54	93.45
NMA1-10	621.8	55.15	57.95	72.24	99.76	73.39	77.11	56.20
NMA1-11	459.0	25.34	32.26	22.80	40.45	32.52	36.11	13.21

Sample Name	Median Hardness	Measured UCS	Freimuth 2021	Meulenkamp 1997	Verwaal and Mulder 1993	Lee et al., 2014	Aoki and Matsukura, 2008	Zahm and Enderlin, 2010
NMA1-12	381.1		24.37	11.25	23.27	22.03	22.69	-7.36
NMA1-14	673.8	86.10	69.88	98.02	126.67	95.18	94.26	69.94
NMA1-15	601.6	73.46	53.90	63.75	90.46	66.36	71.02	50.89
NMA1-16	618.6	48.59	57.30	70.87	98.27	72.25	76.15	55.38
NMA1-2	522.5		40.54	37.30	59.47	44.68	49.92	29.98
NMA1-3	233.9		14.34	1.76	5.45	10.55	6.69	-46.26
NMA1-5	599.0	53.63	53.40	62.70	89.29	65.50	70.25	50.19
NMA1-7	379.0		24.18	11.01	22.89	21.80	22.37	-7.93
NMA1-8	613.5	59.89	56.26	68.66	95.87	70.42	74.58	54.02

Sample Name	Median Hardness	Measured UCS	Freimuth 2021	Meulenkamp 1997	Verwaal and Mulder 1993	Lee et al., 2014	Aoki and Matsukura, 2008	Zahm and Enderlin, 2010
NMA1-8 (Dup.)	660.0	65.62	66.51	90.64	119.14	88.85	89.53	66.31
NMA1-9	497.0	60.34	36.99	30.85	51.25	39.33	44.05	23.25
NMA1-9 (Dup.)	507.5	18.05	38.41	33.40	54.54	41.45	46.42	26.02
NMA2-1	545.4	45.97	44.02	43.90	67.56	50.09	55.57	36.03
OKST1-1	512.3	57.03	39.07	34.60	56.07	42.45	47.51	27.28
OKST1-10	327.3		20.07	6.30	14.79	16.83	15.50	-21.60
OKST1-11	496.9	107.05	36.97	30.82	51.21	39.31	44.03	23.21
OKST1-12	752.5	77.33	92.79	149.20	175.98	141.10	124.27	90.74
OKST1-13	295.5		17.91	4.28	10.92	14.36	12.01	-29.98

Sample Name	Median Hardness	Measured UCS	Freimuth 2021	Meulenkamp 1997	Verwaal and Mulder 1993	Lee et al., 2014	Aoki and Matsukura, 2008	Zahm and Enderlin, 2010
OKST1-14	887.3	307.80	150.72	279.01	287.22	276.78	187.59	126.34
OKST1-15	505.5	36.60	38.13	32.90	53.90	41.04	45.96	25.49
OKST1-17	656.9	73.12	65.76	89.02	117.47	87.48	88.47	65.48
OKST1-18	732.1	44.39	86.23	134.42	162.18	127.44	116.03	85.36
OKST1-2	705.4	45.25	78.31	116.69	145.19	111.48	105.72	78.29
OKST1-3	697.4	53.49	76.09	111.74	140.34	107.11	102.74	76.18
OKST1-4	782.5	130.56	103.37	173.09	197.67	163.94	137.03	98.67
OKST1-5	717.0	70.28	81.66	124.17	152.42	118.15	110.13	81.36
OKST1-6	481.3	87.53	34.95	27.29	46.57	36.35	40.65	19.09

Sample Name	Median Hardness	Measured UCS	Freimuth 2021	Meulenkamp 1997	Verwaal and Mulder 1993	Lee et al., 2014	Aoki and Matsukura, 2008	Zahm and Enderlin, 2010
OKST1-7	700.1	54.23	76.84	113.42	142.00	108.59	103.76	76.91
OKST1-8	581.3	56.07	50.09	55.93	81.65	59.93	65.16	45.50
OKST1-9	673.3	37.36	69.76	97.75	126.39	94.94	94.09	69.81
TXBB1-1	941.8	215.79	183.39	349.94	342.94	363.49	217.74	140.73
TXBB1-2	923.9	65.31	171.96	325.36	323.94	332.41	207.55	136.01
TXBB1-3	911.1	94.87	164.25	308.63	310.82	311.88	200.46	132.64
TXDA1-1	392.6	13.15	25.40	12.59	25.42	23.34	24.44	-4.33
TXDA1-2	463.3	28.57	32.75	23.61	41.58	33.22	36.95	14.33
TXDA1-3	407.9	17.32	26.83	14.56	28.47	25.19	26.88	-0.30

Sample Name	Median Hardness	Measured UCS	Freimuth 2021	Meulenkamp 1997	Verwaal and Mulder 1993	Lee et al., 2014	Aoki and Matsukura, 2008	Zahm and Enderlin, 2010
TXPK1-1	679.8	117.33	71.41	101.38	130.06	98.08	96.37	71.52
TXPK1-2	624.0	82.87	58.42	73.24	100.83	74.22	77.81	56.80
TXPK1-3	607.1	64.08	54.98	65.99	92.94	68.21	72.66	52.34
TXPK1-4	659.8	48.21	66.45	90.51	119.00	88.74	89.44	66.24

Vita

Personal Background	Clayton Reinhard Freimuth Dallas, Texas Son of Reinhard and Paula Freimuth Brother to Isabel and Robert Freimuth
Education	Bachelor of Science, Earth Science, 2015, Frostburg State University
	Master of Science, Geology, 2021 Texas Christian University
Experience	Exploration Intern, Newmont Mining Corp., Summer 2020
	Mudlogger/LWD Engineer, Nabors Drilling Solutions, Oct. 2018 – Aug. 2019
	Mudlogger, Nabors Drilling Solutions, Jan. 2017 – April 2017
	Mudlogger, Exlog, Oct. 2016 – Jan. 2017
	Exploration Intern, Roy Guffey Oil Co., July 2015 – April 2016

Abstract

DETERMINING LEEB HARDNESS AND ITS CONTROLLING FACTORS TO ASSESS THE STRENGTH OF SEDIMENTARY ROCKS

Clayton Reinhard Freimuth, M.S., 2021
Department of Geological Sciences
Texas Christian University

Dr. Helge Alsleben, Associate Professor of Geology

Hardness, defined as resistance to surface deformation, is intrinsic to all materials including sedimentary rocks. The variables controlling sedimentary rock hardness are not completely understood. By understanding these factors, we may better understand related rock strength. Rock strength, defined as a rock's resistance to brittle failure under loading, is important to many industries such as mining, civil engineering, and petroleum exploration.

Rock strength is typically quantified by triaxial load cell tests, which are expensive, time consuming, and require substantial investment in laboratory setup. To circumvent this, other devices have been employed to determine rock strength. For example, the Proceq Equotip Bambino micro-rebound hammer (Bambino) has been used for decades to test the hardness of manmade materials, and to determine strength. Geologic studies empirically correlate Bambino-derived hardness (called Leeb hardness) and uniaxial compressive strength (UCS). However, significant scatter in the data suggest that certain intrinsic (e.g., density) or extrinsic factors (e.g., sample volume) need to be considered for a better correlation.

In this study, I examined relations between Leeb hardness and UCS values, accounting for properties such as: lithology, bulk mineralogy, water loss, volume, density, and effective porosity. Intrinsic properties such as bulk mineralogy, density, effective porosity, and water content correlate with Leeb hardness. Also, sample UCS is related to its density, effective porosity, and mechanical hardness. Ultimately, this study validates previous studies and sheds insight on the controlling properties of a rock's hardness and strength.